

## **Phosphorylation of eIF2 $\alpha$ is a Translational Control Mechanism Regulating Muscle Stem Cell Quiescence and Self-Renewal**

Victoria Zismanov, Victor Chichkov, Veronica Colangelo, Solène Jamet, Shuo Wang,  
Alasdair Syme, Antonis E. Koromilas, and Colin Crist

Cell Stem Cell (2015) Available online 5 November 2015, Published: November 5, 2015

[doi:10.1016/j.stem.2015.09.020](https://doi.org/10.1016/j.stem.2015.09.020)

# Phosphorylation of eIF2 $\alpha$ is a Translational Control Mechanism Regulating Muscle Stem Cell Quiescence and Self-Renewal

Victoria Zismanov,<sup>1,2,†</sup> Victor Chichkov,<sup>1,2,†</sup> Veronica Colangelo<sup>1,2,3,†</sup>, Solène Jamet,<sup>1</sup> Shuo Wang,<sup>1</sup> Alasdair Syme,<sup>1,4</sup> Antonis E. Koromilas,<sup>1,4</sup> and Colin Crist<sup>1,2,\*</sup>

<sup>1</sup>Lady Davis Institute for Medical Research, Jewish General Hospital, Montreal, Quebec, H3T 1E2, Canada.

<sup>2</sup>Department of Human Genetics, McGill University, Montreal, Quebec, H3A 1B1, Canada

<sup>3</sup>Department of Health Sciences, University of Milan Bicocca, Monza, 20900, Italy

<sup>4</sup>Department of Oncology, McGill University, Montreal, Quebec, H2W 1S6, Canada.

\*Correspondence to: colin.crist@mcgill.ca

†These authors contributed equally to this work.

## SUMMARY

Regeneration of adult tissues depends on somatic stem cells that remain quiescent, yet are primed to enter a differentiation program. The molecular pathways that prevent activation of these cells are not well understood. Using mouse skeletal muscle stem cells as a model, we show that a general repression of translation, mediated by the phosphorylation of translation initiation factor eIF2 $\alpha$  at serine 51 (P-eIF2 $\alpha$ ), is required to maintain the quiescent state. Skeletal muscle stem cells unable to phosphorylate eIF2 $\alpha$  exit quiescence, activate the myogenic program and differentiate, but do not self-renew. P-eIF2 $\alpha$  ensures in part the robust translational silencing of accumulating mRNAs that is needed to prevent the activation of muscle stem cells.

Additionally, P-eIF2 $\alpha$  dependent translation of mRNAs regulated by upstream open reading

frames (uORFs) contributes to the molecular signature of stemness. Pharmacological inhibition of eIF2 $\alpha$  dephosphorylation enhances skeletal muscle stem cell self-renewal and regenerative capacity.

## INTRODUCTION

Adult tissues with regenerative potential harbour stem cells that are primed to enter a differentiation program, while remaining quiescent (Simons and Clevers, 2011). These properties are illustrated by skeletal muscle stem cells, which are named ‘satellite cells’ for their position underneath the basal lamina of myofibres (Mauro, 1961), and are essential for all post-natal growth and repair of skeletal muscle (Lepper et al., 2011; McCarthy et al., 2011; Murphy et al., 2011; Sambasivan et al., 2011). Satellite cells and the skeletal muscle progenitor cells that are present during development commonly express members of the paired homeodomain family of transcription factors, Pax3 and/or Pax7 (Relaix et al., 2006). During development, Pax3/Pax7 are important regulators of myogenic progenitor survival, and are required to activate the expression of myogenic determination genes *Myf5* and *MyoD*, with consequent rapid muscle differentiation (Relaix et al., 2005).

Two poorly understood features distinguish satellite cells from their embryonic counterparts. First, satellite cells remain quiescent for long periods of time and only activate the myogenic program in response to damage. During quiescence, satellite cells must ensure their survival and tissue identity, yet the molecular mechanisms that underlie these properties are unknown. Second, satellite cells are primed to activate the myogenic program (Pallafacchina et al., 2010) with the majority of these cells having already activated the expression of *Myf5* (Kuang et al., 2007). The paradoxical nature of these two features can be reconciled by the

microRNA pathway, which prevents the translation of transcripts for *Myf5* (Crist et al., 2012) and also for *Dek* (Cheung et al., 2012), thereby ensuring quiescent satellite cells do not activate the myogenic program or the cell cycle, respectively. Furthermore, some transcripts, such as those for *Myf5*, are sequestered in RNA granules present in the quiescent satellite cell. Upon satellite cell activation, the RNA granules dissociate, *Myf5* transcripts return to polysomes and Myf5 protein rapidly accumulates (Crist et al., 2012).

RNA granules in the quiescent satellite cell share features with stress granules (Buchan and Parker, 2009; Crist et al., 2012), which are large aggregates composed of translation initiation factors, RNA binding proteins and mRNAs. Cells under various forms of stress store mRNAs in stress granules and release them for translation after the stress is resolved. This transition can be regulated by phosphorylation of the alpha ( $\alpha$ ) subunit of eukaryotic initiation factor 2 (eIF2) at serine 51 (S51) (Buchan and Parker, 2009). Phosphorylation of this residue prevents the catalysis of GDP to GTP needed to recycle eIF2-GTP-Met-tRNA ternary complexes, which underlies a decrease in translation reinitiation (Koromilas, 2015).

## RESULTS

### **eIF2 $\alpha$ is Phosphorylated in the Quiescent Satellite Cell**

We asked whether phosphorylation of eIF2 $\alpha$  underlies RNA granule assembly in the quiescent satellite cell. We used antibodies against Pax7 and phospho-eIF2 $\alpha$  (P-eIF2 $\alpha$ ) on single myofibres isolated from *extensor digitorum longus* (EDL) muscle of wild-type mice. Quiescent satellite cells expressing Pax7 were also marked by P-eIF2 $\alpha$  (Figure 1A and 1B). Culture of single EDL myofibres for 6 hours, a duration that is sufficient for activation of the myogenic program (Crist et al., 2012) resulted in the loss of P-eIF2 $\alpha$  in satellite cells expressing

Pax7 or MyoD (Figure 1A and 1B). After culture of myofibres for 24 hours, when satellite cells typically undergo their first cell division, a fraction of Pax7 expressing cells, but not MyoD expressing cells, have P-eIF2 $\alpha$  (Figure 1A and 1B). We used immunoblotting to show that levels of P-eIF2 $\alpha$  are 5-fold higher in satellite cells newly isolated from muscle of adult *Pax3<sup>GFP/+</sup>* mice than after 3 day culture when the majority of satellite cells have typically activated the myogenic program (Figure 1C). Immunofluorescence of satellite cells after 3 day culture show that levels of P-eIF2 $\alpha$  detected by immunoblotting are from a fraction of cells maintaining Pax7-expression that are also positive for P-eIF2 $\alpha$ . Conversely, P-eIF2 $\alpha$  is not detected in satellite cells that have activated the myogenic program and express MyoD (Figure 1D and 1E).

We went on to examine eIF2 $\alpha$  phosphorylation in the quiescent satellite cell, focusing on PKR-like endoplasmic reticulum (ER) kinase (PERK), since it is one of four kinases that phosphorylate eIF2 $\alpha$  in response to stress, it has a mainly pro-survival function (Koromilas, 2014), and plays an important role in maintaining the integrity of adult stem cell pools (van Galen et al., 2014). Cell lysates of newly isolated satellite cells from muscle of adult *Pax3<sup>GFP/+</sup>* mice contain high levels of P-PERK, compared to lysates of activated satellite cells after 3 day culture *ex vivo* (Figure 1F and 1G).

Phosphorylation of eIF2 $\alpha$  leads to a global arrest of translation, but paradoxically, transcripts for Activating Transcription Factor 4 (*ATF4*) and C/EBP Homology Protein (*CHOP*), also known as GADD153, are selectively translated due to upstream open reading frames (uORF) present within their 5' untranslated region (UTR). P-eIF2 $\alpha$  mediated ribosome bypass of these uORFs facilitates *ATF4* and *CHOP* mRNA translation (Palam et al., 2011; Vattem and Wek, 2004). Newly isolated satellite cells accumulate ATF4 and CHOP protein, and their expression is down-regulated in activated satellite cells after 3 day culture (Figure 1F and 1G).

Together, PERK, P-eIF2 $\alpha$  and ATF4 are master regulators of the unfolded protein response (UPR) (Walter and Ron, 2011). We therefore confirmed high levels of the pro-survival UPR target chaperone protein BiP, also known as GRP78, in newly isolated satellite cells, compared to activated cells after 3 day culture (Figure 1F and 1G).

### **Satellite Cells Unable to Phosphorylate eIF2 $\alpha$ Break Quiescence and Activate the Myogenic Program**

We therefore investigated whether eIF2 $\alpha$  phosphorylation plays a role in maintaining the quiescent state of the satellite cell. Since eIF2 $\alpha$  is phosphorylated at S51, we examined satellite cells in the muscle of mice homozygous for a S51 switch to alanine (*eIF2 $\alpha$ <sup>S51A/S51A</sup>*). The perinatal lethality of *eIF2 $\alpha$ <sup>S51A/S51A</sup>* homozygosity is rescued by a transgene encoding the ORF for wild-type eIF2 $\alpha$  flanked by two loxP sites, followed by a second ORF encoding GFP (Back et al., 2009). We crossed these mice with *Pax7<sup>CreERT2/+</sup>* mice (Murphy et al., 2011), such that tamoxifen (tmx) treatment of progeny would result in Pax7-positive (+) satellite cells unable to phosphorylate eIF2 $\alpha$  (hereinafter S51A satellite cells) with coordinate expression of GFP (Figure 2A and 2B). After 5 daily doses of tmx, satellite cells associated with single EDL myofibres had reduced numbers of p54/RCK(+) RNA granules (Figure 2C and 2D) and increased rates of protein synthesis, indicated by incorporation of the puromycin analog O-propagyl-puromycin (OPP), (Figure 2E and 2F). Immunofluorescence on transverse sections of *tibialis anterior* (TA) muscle showed that 79% of Pax7(+) cells had activated the expression of GFP. In addition, GFP(+) cells were found within the interstitial space between muscle fibres (Figure 2G and 2H). Since *Pax7*-expression specifically marks satellite cells (Seale et al., 2000) and cre-mediated recombination in the muscle of *Pax7<sup>CreERT2/+</sup>* mice is specific to Pax7 cells (Murphy et al., 2011), these GFP(+) cells should be progeny of activated satellite cells. To demonstrate activation of the

myogenic program, we show that GFP(+) cells accumulate MyoD (Figure 2I and 2J). As a further indicator of activation, we isolated GFP(+) cells by flow cytometry and used immunoblotting to identify Myf5 protein, which is not accumulated in quiescent satellite cells (Figure 2K). Furthermore, Pax7(+) cells were found outside the basal lamina of muscle fibres (Figure 2L and 2M). S51A satellite cells break quiescence and proliferate as indicated by 5-ethyl-2'-deoxyuridine (EdU) incorporation (Figure 2N and 2O).

To confirm PERK as the kinase that phosphorylates eIF2 $\alpha$  in the quiescent satellite cell, we examined satellite cells after the conditional inactivation of *PERK* (Zhang et al., 2006). Tamoxifen treatment of *Pax7<sup>CreERT2/+</sup>; tg(actb-eIF2 $\alpha^fl$ -GFP); PERK<sup>*fl/fl*</sup>* mice (Figure S1A to S1C) caused satellite cells to a) lose P-PERK, P-eIF2 $\alpha$  (Figure S1D), b) activate the myogenic program (Figure S1E and S1F) and c) exit their normal position underneath the basal lamina (Figure S1G and S1H).

We hypothesize that phosphorylation of eIF2 $\alpha$  has an additional biological role to maintain properties of somatic stem cells through the selective translation of transcripts for stem cell specific genes. We compared quiescent satellite cell gene expression at the level of transcription (Pallafacchina et al., 2010) and translation (Zhang et al., 2015), with transcripts found to be selectively translated when eIF2 $\alpha$  is phosphorylated (Baird et al., 2014). We identified 35 transcripts (Figure 3A, see also Table S1), of which *Usp9x*, *Chd4* (also known as *Mi-2 $\beta$* ), *Stat3*, *Sf3b1*, and *Ddb1* (Blanpain et al., 2004; Cang et al., 2007; Ivanova et al., 2002; Matsunawa et al., 2014; Ramalho-Santos et al., 2002; Tierney et al., 2014; Yoshida et al., 2008) are highlighted (Figure 3A) because they potentially impart upon the satellite cell stem cell properties to self-renew and/or remain quiescent but poised to rapidly enter the myogenic program. In addition, transcripts for *Usp9x* and *Chd4* have 5'UTRs with uORFs (Figure 3A).

We focused on the substrate specific deubiquitylating enzyme *Usp9x* because a) it has 5 conserved uORFs within its 5'UTR and b) *Usp9x* expression is upregulated in mouse embryonic, hematopoietic, neural (Ivanova et al., 2002; Ramalho-Santos et al., 2002) and epithelial stem cells located within the hair follicle bulge (Blanpain et al., 2004). We show that *Usp9x* protein accumulates in wild-type satellite cells, but at lower levels in S51A satellite cells (Figure 3B to 3D). The efficiency of translation of *Usp9x* and *Atf4* is dependent on P-eIF2 $\alpha$ , demonstrated by their shift towards light fractions in S51A satellite cells (Figure S2A and S2B).

We next asked whether microRNA or RNA binding protein mediated silencing of specific transcripts in the quiescent satellite cell is further mediated by the limiting eIF2-GTP-Met-tRNA complexes available to initiate translation when eIF2 $\alpha$  is phosphorylated. We examined transcripts for *MyoD* (suppressed by the RNA binding protein TTP) (Hausburg et al., 2015), *Myf5* (Crist et al., 2012) and *Dek* (Cheung et al., 2012) (suppressed by the microRNA pathway). These transcripts are associated with light fractions in wild-type satellite cells and heavy polysome associated fractions in S51A satellite cells (Figure S2C). Transcripts for *Pax7* and *Actb* are resistant to eIF2 $\alpha$  phosphorylation, since they are present in heavy polysome fractions of both wild-type and S51A satellite cells (Figure S2D).

We addressed the long-term fate of activated S51A satellite cells. Expected outcomes would include a) their continued differentiation along the myogenic program to contribute to new myofibres b) their eventual cell death due to their inability to respond to stress, or c) their eventual return to quiescence by compensatory mechanisms. To test these outcomes, we examined satellite cell fate 10 days after tmx administration. Using immunofluorescence on transverse sections of TA muscle, we show that activated GFP(+) S51A satellite cells give rise to numerous new GFP(+) myofibres, marked by their smaller size, central nucleation and

expression of embryonic myosin heavy chain (embMHC) (Figure 4A and 4B; see also Figure S3A to S3C). At this timepoint, activated satellite cells marked by Pax7 or MyoD both express GFP (Figure 4A and 4C, see also Figure S3D). GFP(+) S51A satellite proliferate prior to their differentiation into myofibres, as indicated by BrdU labeling of central nucleated, GFP(+) myofibres (Figure S3E).

Since disrupting eIF2 $\alpha$  phosphorylation caused satellite cells to emerge from quiescence, activate the myogenic program and contribute to new myofibres, we reasoned that S51A satellite cells should have limited ability to self-renew, which would be indicated by their return to the normal position underneath the basal lamina. To test this *in vivo*, we examined satellite cell behaviour 21 days after tmx administration. S51A satellite cells did not contribute to self-renewal, exhibited by the absence of Pax7, GFP(+) cells (Figure 4D). Conversely, GFP(+) myofibres of tmx treated *Pax7<sup>CreERT2/+</sup>; eIF2 $\alpha$ <sup>S51A/S51A</sup>; tg(actb-eIF2 $\alpha^fl$ -GFP)* remained central nucleated but were growing larger, suggesting that satellite cell contribution to myofibre size and regeneration is not affected by the inability to phosphorylate eIF2 $\alpha$  (Figure 4D and 4E).

We injured TA muscle of tmx treated mice by intramuscular injection of cardiotoxin (ctx), a snake venom toxin that induces muscle fibre necrosis without affecting the viability of satellite cells (Couteaux et al., 1988). Ten days after injury, activated GFP(+) S51A satellite cells had contributed GFP fluorescence to all skeletal muscle fibres within the injured TA muscle (Figure 4F, see also Figure S3A). At this time after ctx injury, when proliferating myoblasts are still present, many of the Pax7 satellite cells present within the injured area were also GFP(+) (Figure 4F). However the absence of Pax7(+), GFP(+) cells 21 days after injury confirms a defect in self-renewal. (Figure 4G and 4H).

Since the PERK P-eIF2 $\alpha$  arm of the UPR protects cells from apoptosis, we next asked if the defect in self-renewal is related to satellite cell survival. While satellite cells unable to phosphorylate eIF2 $\alpha$  are more apoptotic when challenged with the ER stress inducer thapsigargin (Figure S3F to S3G), an increase in apoptotic S51A satellite cells was not observed in the absence of stress *in vivo*, nor after ctx injury (Figure S3H to S3I).

It remained possible that S51A satellite cells retain limited capacity to self-renew and return to quiescence, perhaps by unknown compensatory mechanisms, but were outcompeted by the on average 21% of satellite cells that did not undergo the Cre-mediated excision of the wild-type eIF2 $\alpha$  ORF after tmx treatment and remain GFP-negative (-) (Figure 2H). To rule out this possibility, we compared the self-renewal capacity of 5000 satellite cells isolated from the muscle of tmx treated *eIF2 $\alpha$ <sup>+/+</sup>* (*Pax7<sup>CreERT2/+</sup>*; *eIF2 $\alpha$ <sup>+/+</sup>*; *tg(actb-eIF2 $\alpha$ <sup>fl</sup>-GFP)*) and *eIF2 $\alpha$ <sup>S51A/S51A</sup>* (*Pax7<sup>CreERT2/+</sup>*; *eIF2 $\alpha$ <sup>S51A/S51A</sup>*; *tg(actb-eIF2 $\alpha$ <sup>fl</sup>-GFP)*) donor mice after their engraftment into TA muscle of immunocompromised *Foxn1<sup>nu/nu</sup>* nude mice. Prior to engraftment, the endogenous satellite cells in TA muscle of recipient mice were efficiently ablated with 18 Gray (Gy) hindlimb irradiation (Figure S4A and S4B). 21 days after engraftment, immunofluorescence analysis of transverse sections of engrafted TA muscle indicates that wild-type (*eIF2 $\alpha$ <sup>+/+</sup>*) and S51A donor satellite cells both give rise to numerous GFP(+) muscle fibres (Figure S4C). However, S51A donor satellite cells showed poor capacity to self-renew after engraftment, as shown by reduced numbers of Pax7(+), GFP(+) donor cells (Figure S4C and S4D).

Our *in vivo* results indicate a central role for the phosphorylation of eIF2 $\alpha$  for satellite cell quiescence and self-renewal, while it is not required for satellite cell activation of the myogenic program and differentiation. To confirm these observations, we compared the

activities of isolated wild-type and S51A satellite cells after *ex vivo* culture. Immunofluorescence labeling with antibodies against Pax7 and MyoD shows the loss of Pax7(+), MyoD(-) ‘reserve cells’ that do not activate the myogenic program after 4 days culture (Figure S4E and S4F). However, immunofluorescence labeling of satellite cell cultures with antibodies against the myogenic differentiation factor Myogenin (MyoG) and muscle differentiation marker TroponinT show that S51A satellite cells are still capable of differentiation into multinucleated myotubes (Figure S4G and S4H).

### **Inhibition of eIF2 $\alpha$ Dephosphorylation by the Small Molecule Sal003 Promotes Satellite Cell Self-Renewal During *ex vivo* Culture**

We then examined whether inhibition of eIF2 $\alpha$  dephosphorylation would delay the activation of the myogenic program during *ex vivo* culture. We isolated satellite cells from muscle of adult *Pax3<sup>GFP/+</sup>* mice and cultured them under normal conditions, or in the presence of sal003 (Costa-Mattioli et al., 2007), a potent derivative of salubrinal that blocks the activity of the eIF2 $\alpha$  phosphatase Gadd34/PP1 (Boyce et al., 2005). After 4 days in culture, we immunolabeled satellite cells with antibodies against Pax7 and MyoD. Culture in the presence of 10 $\mu$ M sal003 for 4 days resulted in a 3-fold increase in the numbers of Pax7(+)MyoD(-) cells that have not yet entered the myogenic program and a 2-fold decrease in the numbers of differentiating Pax7(-)MyoD(+) cells (Figure 5A and 5B), which coincides with increased levels of P-eIF2 $\alpha$  (Figure 5C to 5D) and decreased levels of protein synthesis (Figure 5F). Immunoblotting of cell lysates with antibodies against Pax7 and MyoG confirm the effect of sal003 to delay satellite cell entry into the myogenic program during *ex vivo* culture (Figure 5G). In contrast to Pax7 protein levels, there was only a modest and insignificant increase in *Pax7*

mRNA levels from cells cultured in the presence of sal003. Conversely, *MyoG* mRNA levels remained low in satellite cells cultured in the presence of sal003 (Figure 5H).

Sal003 treated cultures are initially marked by low proliferation, but maintain higher rates of proliferation after 3 and 4 days in culture (Figure S5A). The low numbers of apoptotic cells under normal culture conditions was further reduced in the presence of sal003 (Figure S5B) and in total, myogenic colonies were similar in size after 4 days in culture (Figure S5C). Sal003 is not able to increase numbers of cultured S51A satellite cells that are Pax7(+)MyoD(-) (Figure S5D and S5E) nor if added to wild-type satellite cell cultures after 3 days (Figure S5F), when P-eIF2 $\alpha$  levels are low (Figure 1C and 1D). To test whether sal003 permanently prevented or transiently delayed satellite cell activation of the myogenic program, we extended our analysis to longer timepoints. Initial expansion of the satellite cell population delays the activation of the myogenic program but eventually leads to larger, polynucleated myotubes, determined by immunofluorescence with antibodies against MyoG and TroponinT after 5 days culture (Figure S5G and S5H). When added at day 3 in culture, sal003 initially delays differentiation (Figure S5F) but larger, polynucleated myotubes are not observed after 5 days in culture (Figure S5I and S5J). If sal003 is added at day 0 and again at day 3, differentiation of satellite cells into TroponinT(+), polynucleated myotubes does not occur at day 5 (Figure S5K).

### **Sal003 Maintains the Regenerative Capacity of Cultured Satellite Cells**

The robust regenerative capacity of satellite cells is normally lost after *ex vivo* expansion under normal culture conditions (Gilbert et al., 2010; Montarras and Buckingham, 2005). We were thus interested to determine if satellite cells expanded *ex vivo* in the presence of sal003 retain their stem cell properties to self renew and regenerate muscle after engraftment into a mouse model of Duchenne muscular dystrophy (*Dmd*<sup>*mdx*</sup>). Satellite cells were isolated from the

muscle of *Pax3<sup>GFP/+</sup>* mice constitutively expressing firefly luciferase (*Pax3<sup>GFP/+</sup>; tg(actb-luc)*) and cultured for 4 days in the presence of sal003. After this period of *ex vivo* culture, cells were engrafted into TA muscle of 18 Gy irradiated hindlimbs of *Dmd<sup>mdx</sup>; Foxn1<sup>nu/nu</sup>* immunodeficient mice (Figure 6A). Since newly isolated satellite cells typically have higher regenerative capacity than cultured cells (Montarras and Buckingham, 2005; Sacco et al., 2008), we compared engraftment of 10000 cultured donor satellite cells to 10000 and 1600 newly isolated donor satellite cells, the latter corresponding to the number of cells needed to give rise to 10000 cells after 4 days culture in the presence of sal003. We used *in vivo* imaging to quantitatively measure over time the bioluminescence from engrafted donor satellite cells (Gilbert et al., 2010; Sacco et al., 2008). The highest bioluminescence signals were obtained from engrafted cells that had been newly isolated or had been cultured in the presence of sal003. Engraftment of 10000 sal003 treated satellite cells resulted in higher bioluminescence signals than with the same number of control cultured cells and indeed was higher than that obtained with 1600 newly isolated satellite cells (Figure 6B and 6C), demonstrating the advantage of expanding the population in culture under these conditions.

We next examined whether engrafted donor cells isolated from muscle of *Pax3<sup>GFP/+</sup>; tg(actb-luc)* mice retained two functional properties of adult stem cells, self-renewal and differentiation, after *ex vivo* expansion in the presence of sal003. Engraftment of 10000 sal003 treated satellite cells resulted in higher numbers of dystrophin(+) myofibres (Figure 6D and 6F) and Pax7(+), GFP(+) satellite cells of donor origin (Figure 6E and 6G), than 1600 newly isolated satellite cells. Donor cells of *Pax3<sup>GFP/+</sup>* origin that had been cultured in the presence of sal003 were re-isolated by flow cytometry and were confirmed to differentiate into MyoG(+), TroponinT(+) myotubes after 5 days culture (Figure 6H).

## DISCUSSION

A unique feature of many adult stem cells is their existence in a quiescent state until they are activated in response to regenerate tissue (Simons and Clevers, 2011). Adult stem cells require tight regulation of translation, with increased or decreased rates of translation impairing stem cell function (Signer et al., 2015). Our results provide new insight into mechanisms that regulate translation to hold satellite cells in a quiescent state. Specifically, while looking into the mechanisms of RNA granule assembly in the quiescent satellite cell (Crist et al., 2012), we found that translation initiation factor eIF2 $\alpha$  is phosphorylated in the quiescent satellite cell and is rapidly dephosphorylated when satellite cells are activated to enter the myogenic program.

Cells phosphorylate eIF2 $\alpha$  in response to stress to lower rates of translation as an adaptive mechanism to preserve cell function and survival. Adult stem cells likely accumulate stress over long periods of quiescence and therefore require mechanisms to adapt and survive. Quiescent satellite cells adapt to oxidative stress by activating genes required to remove reactive oxygen species (ROS) (Pallafacchina et al., 2010) as well as genes for chelating metals, such as iron and copper, required for redox reactions (Fukada et al., 2007; Pallafacchina et al., 2010). The activation of oxidative stress genes is linked to the UPR because ER enzyme systems that form disulfide bonds during protein folding also generate ROS (Harding et al., 2003). We therefore show the activation of PERK, the kinase that phosphorylates eIF2 $\alpha$  in response to oxidative and ER stress, in the quiescent satellite cell. UPR target genes *ATF4*, *CHOP* and *BiP*, which are required to ensure cell survival and resolve ER stress, are also activated in the quiescent satellite cell. *CHOP* is an *ATF4* target gene and consequently activates gene expression programs important to limit stress damage, or alternatively, initiate apoptosis (Harding et al., 2003; Palam

et al., 2011). CHOP is also a repressor of *MyoD* transcription and its down-regulation is required for C2C12 myoblasts to activate the myogenic differentiation program (Alter and Bengal, 2011).

Interestingly, S51A satellite cells are not more susceptible to apoptosis *in vivo*, but rather break quiescence and activate the myogenic program while losing stem cell capacity to self-renew. We therefore propose an additional role for P-eIF2 $\alpha$  for somatic stem cell properties to self-renew and remain quiescent, mediated by a general repression of translation such that specific mRNAs are silenced or selectively translated.

We show that selective translation of mRNAs regulated by uORFs includes those that are common to a molecular signature for stemness. We highlight the P-eIF2 $\alpha$  dependent translation of transcripts for the deubiquitylating enzyme *Usp9x*, which contains five conserved uORFs. While the impact of *Usp9x* activity on the satellite cell proteome is not yet clear, *Usp9x* stabilizes Mcl-1 protein, a member of the pro-survival BCL2 family, which is otherwise marked for proteosomal degradation by the action of ubiquitin ligases (Schwickart et al., 2010). *Mcl-1* transcripts are also upregulated in quiescent satellite cells (Pallafacchina et al., 2010), and Mcl-1 activity as an anti-apoptotic factor is required for HSC homeostasis (Opferman et al., 2005).

The general repression of translation caused by P-eIF2 $\alpha$  is expected to create competition for available translation initiation complexes, making microRNA and RNA binding protein mediated silencing platforms more robust. *MyoD*, *Myf5* and *Dek* are among genes that are transcribed in the quiescent satellite cell, but are silenced by translational mechanisms (Cheung et al., 2012; Crist et al., 2012; Hausburg et al., 2015). Preventing eIF2 $\alpha$  phosphorylation in satellite cells results in increased rates of global protein synthesis and the shifting of transcripts for *MyoD*, *Myf5* and *Dek* to heavy polysome-associated fractions.

The small number of adult stem cells limits their widespread use in cell-based therapies. Adult stem cells commonly lose their regenerative capacity during expansion *ex vivo* due to their loss of stem cell ability to self-renew (Delaney et al., 2010; Fares et al., 2014; Gilbert et al., 2010; Montarras and Buckingham, 2005; Sacco et al., 2008). We show that pharmacological inhibition of the eIF2 $\alpha$  phosphatase by the small compound sal003 promotes satellite cell self-renewal at the expense of differentiation. We hypothesized that sal003 treatment of satellite cells during *ex vivo* culture would translate into their increased regenerative capacity after engraftment into a mouse model of Duchenne muscular dystrophy. Satellite cells cultured in the presence of sal003 give rise to more dystrophin positive fibres and more satellite cells undergoing self-renewal than an equivalent number of newly isolated, unexpanded cells. We therefore conclude that sal003 promotes the *ex vivo* expansion of satellite cells retaining regenerative capacity, making sal003 a potential candidate to improve stem cell transplantation.

## **EXPERIMENTAL PROCEDURES**

**Full details are provided in the Supplemental Experimental Procedures.**

### **Mice**

Swiss mice (Charles River) were used for single EDL myofibre isolation. All other mice were maintained on a C57BL/6 background. For engraftment assays immunocompromised 5 to 7 week old *Foxn1<sup>nu/nu</sup>; Dmd<sup>mdx-4cv/mdx-4cv</sup>* females and *Foxn1<sup>nu/nu</sup>; Dmd<sup>mdx-4cv/Y</sup>* males (Jackson Laboratories) were used. Intraperitoneal tmx (Cayman Chemical) injections (2.5mg/day) were administered in corn oil, 30% ethanol to mice for five days. For muscle regeneration, 6-8 week-old mice were anesthetized by isofluorane (CDMV) inhalation and 50 $\mu$ l of 10 $\mu$ M ctx (Sigma) was injected into the TA muscle. At 10 and 21 days following injury, muscles were harvested for

analysis by immunofluorescence. For EdU labeling (Life Technologies), mice received 200µg EdU in 100µl PBS by intraperitoneal injection five times at 8 hour intervals, prior to analysis at day 5 after tmx administration. BrdU (0.8 mg/ml, Sigma) was provided in the drinking water supplemented with 1% sucrose for five days.

### **Cell and Single Fibre Isolation and Culture**

Satellite cells were isolated from abdominal and diaphragm muscle of 5-8 week old *Pax3<sup>GFP/+</sup>* and *Pax3<sup>GFP/+</sup>; tg(actb-luc)* (Taconic) mice or 5-8 week old tmx treated *Pax7<sup>CreERT2/+</sup>*; *eIF2 $\alpha$ <sup>S51A/S51A</sup>*; *tg(actb-eIF2 $\alpha$ <sup>l</sup>-eGFP)* and *Pax7<sup>CreERT2/+</sup>*; *tg(actb-eIF2 $\alpha$ <sup>l</sup>-eGFP)* mice, as previously described (Montarras and Buckingham, 2005) using a FACSAriaIII cell sorter (BD Biosciences). Sorted cells were cultured in 39% DMEM, 39% F12, 20% fetal calf serum (Life Technologies), 2% UltrosorG (Pall Life Sciences), for the times indicated. When indicated, cultures were supplemented with 0.1% dimethylsulfoxide (DMSO control, Sigma), 10µM sal003 (Sigma), 100 µg/ml cycloheximide (CHX), 1 µM thapsigargin (TG, Sigma), 50 µM EdU, 50 µM OPP (Medchem Source). For polysome fractions, satellite cells were isolated with the MACS Satellite Cell Isolation Kit, together with anti-Integrin  $\alpha$ -7 MicroBeads (Miltenyl Biotec) (Figure S3E). Single fibres were isolated by trituration of 0.2% collagenase D (Sigma) treated EDL muscle of adult mice.

### **Immunodetection**

Immunofluorescence labeling of cultured satellite cells, single EDL myofibres and transverse sections of TA muscle was performed as described previously (Crist et al., 2009). Pre-fixation was required for immunolabeling with antibodies against GFP. TAs were fixed for 2 hours in 0.5% paraformaldehyde at 4°C and equilibrated overnight in 20% sucrose at 4°C. Tissues were mounted in Frozen Section Compound (VWR) and flash frozen in a liquid nitrogen cooled

isopentane bath. For immunoblotting, cell lysates were prepared as described previously (Crist et al., 2009). Densitometry of immunoblots was performed with ImageJ. EdU and OPP were detected by Click-IT® Detection kits (Life Technologies). Apoptosis was detected by ApopTag Red In Situ Apoptosis Detection Kit (Millipore).

### **RNA Analysis**

RNA was isolated from cells or polysome fractions with TRIzol reagent (Life Technologies) and treated with DNase (Roche). RNA was reverse transcribed with Superscript III reverse transcriptase (Life Technologies) using oligoDT primers.

### **Statistical Analysis**

Graphical analysis is presented as mean ± standard error of the mean (s.e.m.) or 95% confidence interval, when indicated in the figure legends. Unless otherwise indicated, at least three independent replicates of each experiment were performed. Significance was calculated using unpaired Student's t-tests with two-tailed P values: \*  $p < 0.05$ , \*\*  $p < 0.01$ , \*\*\*  $p < 0.001$ .

### **SUPPLEMENTAL INFORMATION**

**Supplemental Information includes Supplemental Experimental Procedures, five figures, and one table.**

### **AUTHOR CONTRIBUTIONS**

C.C. conceived and designed the study. A.K. provided guidance throughout. V.Z., V.C., V.C., S.J. and C.C. performed experiments and collected data. S.W. provided expertise for sucrose gradient and polysome fractionation. A.S. irradiated mouse hindlimbs. C.C. analyzed data and wrote the paper. V.Z., V.C. and V.C. contributed equally to the study.

### **ACKNOWLEDGEMENTS**

We thank J. Chung for technical help, C. Young for providing assistance with flow cytometry and A. Mouland for assistance with polysome fractionation. R. Kaufman and D. Cavener generously provided *eIF2 $\alpha$ <sup>S51A/S51A</sup>*; *tg(actb-eIF2 $\alpha$ <sup>fl</sup>-GFP)* and *PERK<sup>fl/fl</sup>* mice, respectively. C.C. and co-workers are funded by the Canadian Institute for Health Research (CIHR 286519) the Stem Cell Network and the Muscular Dystrophy Association (351259). A.K. is supported by the CIHR (38160) and the Canadian Cancer Society Research Institute (700886).

## REFERENCES

- Alter, J., and Bengal, E. (2011). Stress-Induced C/EBP Homology Protein (CHOP) Represses MyoD Transcription to Delay Myoblast Differentiation. *PLoS ONE* 6, e29498.
- Back, S.H., Scheuner, D., Han, J., Song, B., Ribick, M., Wang, J., Gildersleeve, R.D., Pennathur, S., and Kaufman, R.J. (2009). Translation Attenuation through eIF2a Phosphorylation Prevents Oxidative Stress and Maintains the Differentiated State in b Cells. *Cell Metab.* 10, 13–26.
- Baird, T.D., Palam, L.R., Fusakio, M.E., Willy, J.A., Davis, C.M., McClintick, J.N., Anthony, T.G., and Wek, R.C. (2014). Selective mRNA translation during eIF2 phosphorylation induces expression of IBTK. *Mol. Biol. Cell* 25, 1686–1697.
- Blanpain, C., Lowry, W.E., Geoghegan, A., Polak, L., and Fuchs, E. (2004). Self-renewal, multipotency, and the existence of two cell populations within an epithelial stem cell niche. *Cell* 118, 635–648.
- Boyce, M., Bryant, K.F., Jousse, C., Long, K., Harding, H.P., Scheuner, D., Kaufman, R.J., Ma, D., Coen, D.M., Ron, D., et al. (2005). A selective inhibitor of eIF2alpha dephosphorylation protects cells from ER stress. *Science* 307, 935–939.
- Buchan, J.R., and Parker, R. (2009). Eukaryotic stress granules: the ins and outs of translation. *Mol. Cell* 36, 932–941.
- Cang, Y., Zhang, J., Nicholas, S.A., Kim, A.L., Zhou, P., and Goff, S.P. (2007). DDB1 is essential for genomic stability in developing epidermis. *Proc. Natl. Acad. Sci. U.S.A.* 104, 2733–2737.
- Cheung, T.H., Quach, N.L., Charville, G.W., Liu, L., Park, L., Edalati, A., Yoo, B., Hoang, P., and Rando, T.A. (2012). Maintenance of muscle stem-cell quiescence by microRNA-489. *Nature* 482, 524–528.
- Costa-Mattioli, M., Gobert, D., Stern, E., Gamache, K., Colina, R., Cuello, C., Sossin, W.,

- Kaufman, R., Pelletier, J., Rosenblum, K., et al. (2007). eIF2 $\alpha$  phosphorylation bidirectionally regulates the switch from short- to long-term synaptic plasticity and memory. *Cell* *129*, 195–206.
- Couteaux, R., Mira, J.C., and d'Albis, A. (1988). Regeneration of muscles after cardiotoxin injury. I. Cytological aspects. *Biol. Cell* *62*, 171–182.
- Crist, C.G., Montarras, D., and Buckingham, M. (2012). Muscle Satellite Cells Are Primed for Myogenesis but Maintain Quiescence with Sequestration of Myf5 mRNA Targeted by microRNA-31 in mRNP Granules. *Cell Stem Cell* *11*, 118–126.
- Crist, C.G., Montarras, D., Pallafacchina, G., Rocancourt, D., Cumano, A., Conway, S.J., and Buckingham, M. (2009). Muscle stem cell behavior is modified by microRNA-27 regulation of Pax3 expression. *Proc. Natl. Acad. Sci. U.S.A.* *106*, 13383–13387.
- Delaney, C., Heimfeld, S., Brashem-Stein, C., Voorhies, H., Manger, R.L., and Bernstein, I.D. (2010). Notch-mediated expansion of human cord blood progenitor cells capable of rapid myeloid reconstitution. *Nat Med* *16*, 232–236.
- Fares, I., Chagraoui, J., Gareau, Y., Gingras, S., Ruel, R., Mayotte, N., Csaszar, E., Knapp, D.J.H.F., Miller, P., Ngom, M., et al. (2014). Cord blood expansion. Pyrimidoindole derivatives are agonists of human hematopoietic stem cell self-renewal. *Science* *345*, 1509–1512.
- Fukada, S.-I., Uezumi, A., Ikemoto, M., Masuda, S., Segawa, M., Tanimura, N., Yamamoto, H., Miyagoe-Suzuki, Y., and Takeda, S. (2007). Molecular signature of quiescent satellite cells in adult skeletal muscle. *Stem Cells* *25*, 2448–2459.
- Gilbert, P.M., Havenstrite, K.L., Magnusson, K.E.G., Sacco, A., Leonardi, N.A., Kraft, P., Nguyen, N.K., Thrun, S., Lutolf, M.P., and Blau, H.M. (2010). Substrate elasticity regulates skeletal muscle stem cell self-renewal in culture. *Science* *329*, 1078–1081.
- Harding, H.P., Zhang, Y., Zeng, H., Novoa, I., Lu, P.D., Calfon, M., Sadri, N., Yun, C., Popko, B., Paules, R., et al. (2003). An integrated stress response regulates amino acid metabolism and resistance to oxidative stress. *Mol. Cell* *11*, 619–633.
- Hausburg, M.A., Doles, J.D., Clement, S.L., Cadwallader, A.B., Hall, M.N., Blackshear, P.J., Lykke-Andersen, J., and Olwin, B.B. (2015). Post-transcriptional regulation of satellite cell quiescence by TTP-mediated mRNA decay. *Elife* *4*.
- Ivanova, N.B., Dimos, J.T., Schaniel, C., Hackney, J.A., Moore, K.A., and Lemischka, I.R. (2002). A stem cell molecular signature. *Science* *298*, 601–604.
- Koromilas, A.E. (2015). Roles of the translation initiation factor eIF2 $\alpha$  serine 51 phosphorylation in cancer formation and treatment. *Biochim. Biophys. Acta* *1849*, 871–880.
- Kuang, S., Kuroda, K., Le Grand, F., and Rudnicki, M.A. (2007). Asymmetric self-renewal and commitment of satellite stem cells in muscle. *Cell* *129*, 999–1010.

- Lepper, C., Partridge, T.A., and Fan, C.-M. (2011). An absolute requirement for Pax7-positive satellite cells in acute injury-induced skeletal muscle regeneration. *Development* 138, 3639–3646.
- Matsunawa, M., Yamamoto, R., Sanada, M., Sato-Otsubo, A., Shiozawa, Y., Yoshida, K., Otsu, M., Shiraishi, Y., Miyano, S., Isono, K., et al. (2014). Haploinsufficiency of Sf3b1 leads to compromised stem cell function but not to myelodysplasia. *Leukemia* 28, 1844–1850.
- Mauro, A. (1961). Satellite cell of skeletal muscle fibers. *J Biophys Biochem Cytol* 9, 493–495.
- McCarthy, J.J., Mula, J., Miyazaki, M., Erfani, R., Garrison, K., Farooqui, A.B., Srikuea, R., Lawson, B.A., Grimes, B., Keller, C., et al. (2011). Effective fiber hypertrophy in satellite cell-depleted skeletal muscle. *Development* 138, 3657–3666.
- Montarras, D., and Buckingham, M. (2005). Direct Isolation of Satellite Cells for Skeletal Muscle Regeneration. *Science* 309, 2064–2067.
- Murphy, M.M., Lawson, J.A., Mathew, S.J., Hutcheson, D.A., and Kardon, G. (2011). Satellite cells, connective tissue fibroblasts and their interactions are crucial for muscle regeneration. *Development* 138, 3625–3637.
- Opferman, J.T., Iwasaki, H., Ong, C.C., Suh, H., Mizuno, S.-I., Akashi, K., and Korsmeyer, S.J. (2005). Obligate role of anti-apoptotic MCL-1 in the survival of hematopoietic stem cells. *Science* 307, 1101–1104.
- Palam, L.R., Baird, T.D., and Wek, R.C. (2011). Phosphorylation of eIF2 Facilitates Ribosomal Bypass of an Inhibitory Upstream ORF to Enhance CHOP Translation. *Journal of Biological Chemistry* 286, 10939–10949.
- Pallafacchina, G., François, S., Regnault, B., Czarny, B., Dive, V., Cumano, A., Montarras, D., and Buckingham, M. (2010). An adult tissue-specific stem cell in its niche: a gene profiling analysis of in vivo quiescent and activated muscle satellite cells. *Stem Cell Res* 4, 77–91.
- Ramalho-Santos, M., Yoon, S., Matsuzaki, Y., Mulligan, R.C., and Melton, D.A. (2002). “Stemness”: transcriptional profiling of embryonic and adult stem cells. *Science* 298, 597–600.
- Relaix, F., Montarras, D., Zaffran, S., Gayraud-Morel, B., Rocancourt, D., Tajbakhsh, S., Mansouri, A., Cumano, A., and Buckingham, M. (2006). Pax3 and Pax7 have distinct and overlapping functions in adult muscle progenitor cells. *J. Cell Biol.* 172, 91–102.
- Relaix, F., Rocancourt, D., Mansouri, A., and Buckingham, M. (2005). A Pax3/Pax7-dependent population of skeletal muscle progenitor cells. *Nature* 435, 948–953.
- Sacco, A., Doyonnas, R., Kraft, P., Vitorovic, S., and Blau, H.M. (2008). Self-renewal and expansion of single transplanted muscle stem cells. *Nature* 456, 502–506.
- Sambasivan, R., Yao, R., Kissenpfennig, A., Van Wittenberghe, L., Paldi, A., Gayraud-Morel, B., Guenou, H., Malissen, B., Tajbakhsh, S., and Galy, A. (2011). Pax7-expressing satellite cells

are indispensable for adult skeletal muscle regeneration. *Development* 138, 4333–4333.

Schwickart, M., Huang, X., Lill, J.R., Liu, J., Ferrando, R., French, D.M., Maecker, H., O'Rourke, K., Bazan, F., Eastham-Anderson, J., et al. (2010). Deubiquitinase USP9X stabilizes MCL1 and promotes tumour cell survival. *Nature* 463, 103–107.

Seale, P., Sabourin, L.A., Girgis-Gabardo, A., Mansouri, A., Gruss, P., and Rudnicki, M.A. (2000). Pax7 is required for the specification of myogenic satellite cells. *Cell* 102, 777–786.

Signer, R.A.J., Magee, J.A., Salic, A., and Morrison, S.J. (2015). Haematopoietic stem cells require a highly regulated protein synthesis rate. *Nature* 508, 49–54.

Simons, B.D., and Clevers, H. (2011). Strategies for homeostatic stem cell self-renewal in adult tissues. *Cell* 145, 851–862.

Tierney, M.T., Aydogdu, T., Sala, D., Malecova, B., Gatto, S., Puri, P.L., Latella, L., and Sacco, A. (2014). STAT3 signaling controls satellite cell expansion and skeletal muscle repair. *Nat Med* 1–7.

van Galen, P., Kreso, A., Mbong, N., Kent, D.G., Fitzmaurice, T., Chambers, J.E., Xie, S., Laurenti, E., Hermans, K., Eppert, K., et al. (2014). The unfolded protein response governs integrity of the haematopoietic stem-cell pool during stress. *Nature* 510, 268–272.

Vattem, K.M., and Wek, R.C. (2004). Reinitiation involving upstream ORFs regulates ATF4 mRNA translation in mammalian cells. *Proc. Natl. Acad. Sci. U.S.A.* 101, 11269–11274.

Walter, P., and Ron, D. (2011). The unfolded protein response: from stress pathway to homeostatic regulation. *Science* 334, 1081–1086.

Yoshida, T., Hazan, I., Zhang, J., Ng, S.Y., Naito, T., Snippert, H.J., Heller, E.J., Qi, X., Lawton, L.N., Williams, C.J., et al. (2008). The role of the chromatin remodeler Mi-2 in hematopoietic stem cell self-renewal and multilineage differentiation. *Genes Dev.* 22, 1174–1189.

Zhang, T., Günther, S., Looso, M., Künne, C., Krüger, M., Kim, J., Zhou, Y., and Braun, T. (2015). Prmt5 is a regulator of muscle stem cell expansion in adult mice. *Nature Communications* 6, 7140.

Zhang, W., Feng, D., Li, Y., Iida, K., McGrath, B., and Cavener, D.R. (2006). PERK EIF2AK3 control of pancreatic beta cell differentiation and proliferation is required for postnatal glucose homeostasis. *Cell Metab.* 4, 491–497.

## FIGURE LEGENDS

**Figure 1. eIF2 $\alpha$  is Phosphorylated in Quiescent Satellite Cells.**

(A) Immunostaining Pax7 (green) or MyoD (green) and P-eIF2 $\alpha$  (red) on newly isolated (0 hr) and cultured (6, 24 hrs) EDL myofibres from wild-type mice. □ Lower panels show merged images with DAPI.

(B) Fraction of Pax7(+) and MyoD(+) nuclei on single myofibres that show immunofluorescence for P-eIF2 $\alpha$  after 0, 6 and 24 hrs of culture.

(C) Immunoblotting against P-eIF2 $\alpha$  and total eIF2 $\alpha$  (eIF2 $\alpha$ ) from cell lysates of newly isolated satellite cells (D0) and after 3 day culture (D3). Relative levels of P-eIF2 $\alpha$ , normalized to total eIF2 $\alpha$  are reported, with a representative immunoblot shown.

(D) Immunostaining for Pax7 (green), MyoD (green) and P-eIF2 $\alpha$  (red) after 3 day culture of satellite cells. Merged images with DAPI are shown.

(E) Quantification of satellite cell nuclei expressing Pax7 or MyoD and P-eIF2 $\alpha$  after 3 day culture of satellite cells.

(F) Representative images of immunoblotting against P-PERK, ATF4, CHOP, BiP and  $\beta$ -tubulin from cell lysates of newly isolated satellite cells (D0) and after 3 day culture (D3).

(G) Relative levels of P-PERK, ATF4, CHOP and BiP, normalized to  $\beta$ -tubulin, are indicated.

All values indicate mean ( $n \geq 3$ )  $\pm$  s.e.m. \*\*\*  $p < 0.001$ . (nd, not detected). Scale bars, 20 $\mu$ m.

**Figure 2. Satellite Cells Unable to Phosphorylate eIF2 $\alpha$  Enter the Myogenic Program *in vivo*.**

(A) A serine to alanine switch at position 51 (S51A) prevents eIF2 $\alpha$  phosphorylation. Mice homozygous for this allele are not viable and are rescued by a transgene with wild-type eIF2 $\alpha$  under the control of CMV enhancer and chicken  $\beta$ -actin promoter (*actb*). The wild-type eIF2 $\alpha$  is flanked by two loxP sites and positioned upstream of a GFP reporter (green). Crossing

this line with a  $Pax7^{CreERT2/+}$  allele, followed by tmx administration, permits the conditional expression of homozygous eIF2 $\alpha$  S51A and GFP (green) in Pax7 satellite cells.

(B) Immunoblotting for P-eIF2 $\alpha$  and total eIF2 $\alpha$  (eIF2 $\alpha$ ) of cell lysates from newly isolated GFP(+) cells from muscle of  $Pax3^{GFP/+}$  (wt) and tmx treated  $Pax7^{CreERT2/+}$ ,  $tg(actb-eIF2a^{fl}-GFP)$ ,  $eIF2\alpha^{S51A/S51A}$  (S51A) animals. The tmx regime and day of analysis are shown. Relative levels of P-eIF2 $\alpha$ , normalized to total eIF2 $\alpha$  are indicated, with representative immunoblots.

(C) Immunostaining for Pax7 (green) and p54/RCK (RCK, red) on isolated EDL myofibres from tmx treated wt ( $Pax7^{+/+}$ ; no Cre) and S51A ( $eIF2\alpha^{S51A/S51A}$ ) mice. □ Lower panels show merged images with DAPI.

(D) Numbers of p54/RCK(+) granules per Pax7 positive satellite cell in (C).

(E) Immunostaining for Pax7 (red) and GFP (green), combined with detection of OPP (far red) on EDL myofibres from tmx treated wt ( $Pax7^{+/+}$ ; no Cre) and S51A ( $eIF2\alpha^{S51A/S51A}$ ) mice. EDL myofibres were also cultured for 6 hours (right panels) or in the presence of cycloheximide (CHX, left panels). Upper panels show merged images with DAPI, overlaid on brightfield to show myofibres.

(F) Rates of protein synthesis, reported by total cell OPP fluorescence in (E).

(G) Immunostaining for Pax7 (red) and GFP (green) on transverse sections of TA muscle after 5 daily doses of tmx (indicated). □ Right panels show merged images with DAPI, which are overlaid on brightfield images of transverse fibre sections. Asterik indicates a Pax7(+), GFP(+) satellite cell. Arrows indicate position of GFP(+) cells between muscle fibres.

(H) Fraction of Pax7(+) nuclei that show immunofluorescence for GFP indicated in (G).

(I) Immunostaining MyoD (red) and GFP (green) on transverse sections of TA muscle after tmx treatment. Right panels are merged images with DAPI, overlaid on brightfield to show myofibres.

(J) Fraction of GFP(+) cells that are MyoD(+) in (I).

(K) Immunoblotting against Myf5 and  $\beta$ -tubulin from cell lysates of newly isolated GFP(+) cells from muscle of *Pax3<sup>GFP/+</sup>* (wt) and tmx treated *Pax7<sup>CreERT2/+</sup>*, *tg(actb-eIF2 $\alpha^{\text{fl}}$ -GFP)*, *eIF2 $\alpha^{\text{S51A/S51A}}$*  (S51A) animals. Relative levels of Myf5 normalized to  $\beta$ -tubulin are indicated, with representative immunoblots shown.

(L) Immunostaining Pax7 (green) and Laminin (Lam, red) on transverse sections of TA muscle after tmx treatment. Right panels show merged images with DAPI. Arrows indicate position of satellite cells outside basal lamina.

(M) Fraction of Pax7(+) nuclei outside the basal lamina of myofibres after tmx treatment indicated in (L).

(N) Representative images of EdU(+) satellite cells isolated from tmx treated *Pax7<sup>CreERT2/+</sup>*, *tg(actb-eIF2 $\alpha^{\text{fl}}$ -GFP)*, *eIF2 $\alpha^{+/+}$*  or *eIF2 $\alpha^{\text{S51A/S51A}}$*  and deposited on slides by cytopsin.

(O) Fraction of EdU(+) satellite cells isolated from tmx treated mice, as indicated in (N).

Scale bars, 50 $\mu\text{m}$  except in (C), 10 $\mu\text{m}$  and (N), 20 $\mu\text{m}$ . All values indicate mean ( $n \geq 3$ )  $\pm$  s.e.m. \*  $p < 0.05$ , \*\*  $p < 0.01$ , \*\*\*  $p < 0.001$ . (nd, not detected).

See also Figure S1.

### **Figure 3. Selective mRNA translation during eIF2 $\alpha$ phosphorylation.**

(A) Venn diagram of the quiescent satellite cell transcriptome (red) and proteome (green) with mRNAs that are selectively translated by P-eIF2 $\alpha$ . 35 genes common to each of the data sets are indicated (see also Table S1), of which 5 are further identified as regulators of stem and/or

progenitor cells. *Usp9x* and *Chd4* transcripts are highlighted (blue) because they have uORFs in the 5'UTR.

(B) Immunostaining Pax7 (green) and *Usp9x* (red) on EDL myofibres isolated from tmx treated wild-type (wt) and S51A mice. □ Lower panels show merged images with DAPI. Scale bar, 10µm. Structure of *Usp9x* transcripts are shown with 5 uORFs.

(C) Fraction of Pax7(+) cells that show immunofluorescence for *Usp9x* indicated in (B). Values indicate mean (n≥3) ± s.e.m. \*\*\*  $p < 0.001$ .

(D) Immunoblotting against *Usp9x* and  $\beta$ -tubulin from cell lysates of newly isolated GFP(+) cells from muscle of tmx treated *Pax7<sup>CreERT2/+</sup>*, *tg(actb-eIF2 $\alpha^fl$ -GFP)*, *eIF2 $\alpha^{+/+}$*  (wt) and *eIF2 $\alpha^{S51A/S51A}$*  (S51A) animals. Relative levels of *Usp9x* normalized to  $\beta$ -tubulin are indicated, with representative immunoblots shown.

See also Figure S2.

**Figure 4. Activated S51A Satellite Cells Contribute to New Muscle Fibres, but not to Self-Renewal *in vivo*.**

(A) Immunostaining Pax7 (red) and GFP (green) on transverse section of uninjured TA muscle. Days of tmx administration (black) and analysis (red) are shown. Arrows indicate the position of Pax7(+) nuclei. Magnified images (right) are provided. Scale bar, 20µm.

(B) Mean cross section area (CSA) of GFP(-) and GFP(+) myofibres of uninjured TA muscle, shown in (A), 10 days after tmx administration. Values indicate mean (n≥500 myofibres from three independent mice) ± 95% confidence interval (c.i.) \*\*\*  $p < 0.001$ .

(C) Fraction of Pax7(+) satellite cells, which are positive for GFP, shown in (A), 10 days after tmx administration. Values indicate mean (n≥3) ± s.e.m. \*  $p < 0.05$ , \*\*\*  $p < 0.001$ , nd, not detected.

(D) Immunostaining Pax7 (red) and GFP (green) on transverse section of uninjured TA muscle.

Days of tmx administration (black) and analysis (red) are shown. Arrows indicate the position of Pax7(+) nuclei. Magnified images (right) are provided. Scale bar, 20 $\mu$ m.

(E) Mean CSA of GFP(-) and GFP(+) myofibres of uninjured TA muscle, shown in (C), 21 days after tmx administration. Values indicate mean ( $n \geq 200$  myofibres from three independent mice)  $\pm$  95% c.i. \*\*  $p < 0.01$ .

(F and G) Immunostaining Pax7 (red) and GFP (green) on transverse section of TA muscle (F) 10 and (G) 21 days after ctx injury. Days of tmx administration (black), ctx injury (blue) and analysis (red) are shown. Arrows indicate the position of Pax7(+) nuclei. Magnified images (right) are provided. Scale bar, 20 $\mu$ m.

(H) Numbers of Pax7(+) satellite cells, per 100 myofibres that are negative (grey) or positive (green) for GFP, shown in (D), 21 days after tmx administration and ctx injury. Values indicate mean ( $n \geq 3$ )  $\pm$  s.e.m. \*  $p < 0.05$ , \*\*\*  $p < 0.001$ , nd, not detected.

See also Figure S3 and S4.

### **Figure 5. Satellite Cell Self-Renewal During *ex vivo* Culture is Enhanced by Sal003.**

(A) Immunostaining Pax7 (green) and MyoD (red) on satellite cells isolated from muscle of *Pax3<sup>GFP/+</sup>* and cultured *ex vivo* with DMSO (control) or sal003 for 4 days. Arrows indicate position of Pax7(+), MyoD(-) reserve cells.

(B) Frequency of cells undergoing self-renewal (Pax7+MyoD-), activation (Pax7+MyoD+) and differentiation (Pax7-MyoD+) after 4 day culture with DMSO (control) or sal003.

(C) Immunoblotting P-eIF2 $\alpha$  and total eIF2 $\alpha$  from cell lysates after 4-day culture in DMSO (control) and sal003. Relative levels of P-eIF2 $\alpha$  normalized to total eIF2 $\alpha$  are indicated, with representative immunoblots.

(D) Immunostaining for Pax7 (green) and P-eIF2 $\alpha$  (red) after 4 day culture of satellite cells in the presence of DMSO (control) or sal003. Merged images with DAPI are shown.

(E) Fraction of Pax7(+) cells that are positive for P-eIF2 $\alpha$  in (D).

(F) OPP incorporation into satellite cells cultured for 4 days in the presence of DMSO (control) or sal003 after 1 hour culture. The mean of n=3 experiments with each experiment including n=3 plates is indicated, with a representative FACS plot shown.

(G) Immunoblotting Pax7, MyoG and  $\beta$ -tubulin from cell lysates after 4-day culture in DMSO (control) and sal003. Relative levels of Pax7 and MyoG, normalized to  $\beta$ -tubulin, are indicated with representative immunoblots.

(H) Relative *Pax7* and *MyoG* mRNA levels, determined by RT-qPCR, after 4-day culture with DMSO (control) and sal003. *Pax7* and *MyoG* mRNA levels are normalized to *actb* and reported relative to control conditions.

Scale bars, 20 $\mu$ m. All values indicate mean (n $\geq$ 3)  $\pm$  s.e.m. ns, not significant, \*  $p$ <0.05 ,

\*\* $p$ <0.01, \*\*\*  $p$ <0.001.

See also Figure S5.

**Figure 6. Satellite Cells Expanded in the Presence of Sal003 Retain Regenerative Stem Cell Capacity to Differentiate and Self-Renew After Intramuscular Engraftment into a Mouse Model of Duchenne Muscular Dystrophy.**

(A) Schematic representation of cell engraftment.

(B) Engraftment of 1600 and 10000 newly isolated satellite cells (D0, black and green circles, respectively) as well as 10000 satellite cells after culture for 4 days in the presence of DMSO (red squares) and sal003 (blue triangles), monitored by bioluminescence imaging for three weeks after engraftment. Results are reported as mean and s.e.m. of total bioluminescence flux (photons/second, p/s) of 6 replicate engraftments. \*  $p < 0.05$ .

(C) Representative images of bioluminescence derived 14 days after engraftment of satellite cells that had been newly isolated from muscle of *Pax3<sup>GFP/+</sup>; tg(actb-luc)* and after 4 day culture in the presence of DMSO and sal003.

(D) Immunostaining Dystrophin (Dys, red) and Pax7 (green) on transverse sections 21 days after engraftment with satellite cells newly isolated (D0) or cultured in the presence of DMSO and sal003 for 4 days. Arrows indicate the location of satellite cells. Areas of engraftment outlined (dotted white line) indicate the location of myofibres (asterisk) associated with satellite cells of donor origin, shown in (E). Scale bar, 50 $\mu$ m.

(E) Immunostaining Pax7 (green) and GFP (red) on adjacent 10 $\mu$ m transverse sections to (D). DAPI(+) nuclei are shown (blue). Bottom panels are merged with brightfield images to show outline of myofibres. Arrows indicate Pax7(+), GFP(+) satellite cells of donor origin. Asteriks indicate identity of myofibres that are dystrophin(+) on (D). Scale bar, 50 $\mu$ m.

(F) Scatterplot indicating numbers of dystrophin(+) myofibres present 21 days after engraftment of 10000 (green) or 1600 (black) newly isolated satellite cells and after 4 day culture in the presence of DMSO (red) or sal003 (blue). Numbers of revertant dystrophin(+) fibres on contralateral TAs that were not engrafted are shown (orange).

(G) Scatterplot indicating numbers of Pax7(+), GFP(+) satellite cells of donor origin per transverse section 21 days after engraftment of 10000 (green) or 1600 (black) newly isolated satellite cells and after 4 day culture in the presence of DMSO (red) or sal003 (blue). Each point on scatterplots shown in (F) and (G) represents an individual engraftment. The mean and s.e.m. are indicated. (10000 newly isolated n=6, 1600 newly isolated n=8, 4 day sal003 n=6, 4 day DMSO n=6; sal003, n=6 and revertant n=16) \*  $p < 0.05$ , \*\*  $p < 0.01$ , \*\*\*  $p < 0.001$ , ns, not significant.

(H) Re-isolation and 5 day culture of sal003 treated, GFP(+) cells, 21 days after engraftment. Immunolabeling MyoG (MyoG, green), TroponinT (TnT, red). Image is shown merged with DAPI nuclear stain (blue). Scale bar, 20 $\mu$ m.

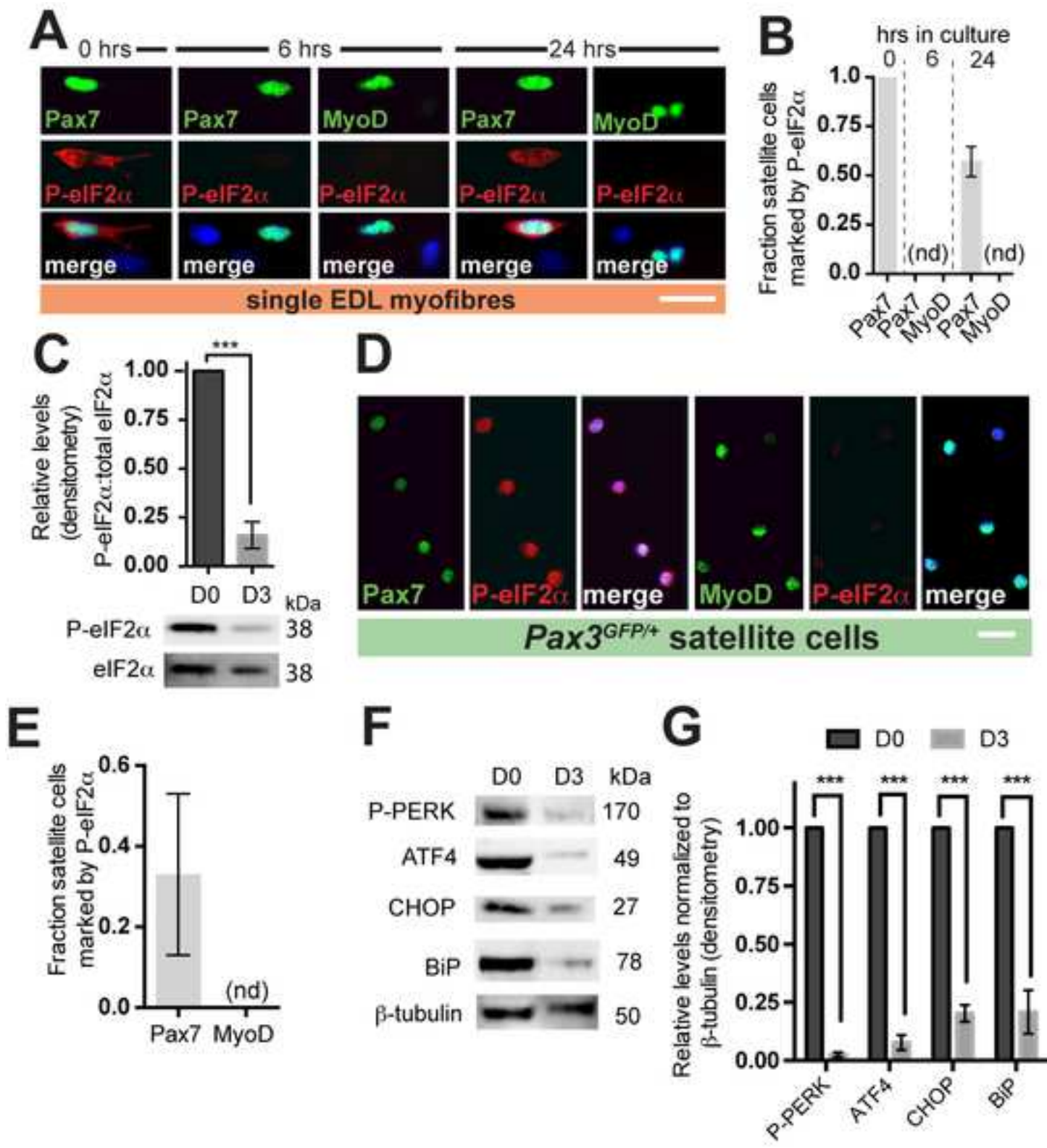


Figure 2  
 Click here to download Figure: Figure2\_revised\_v1.tif

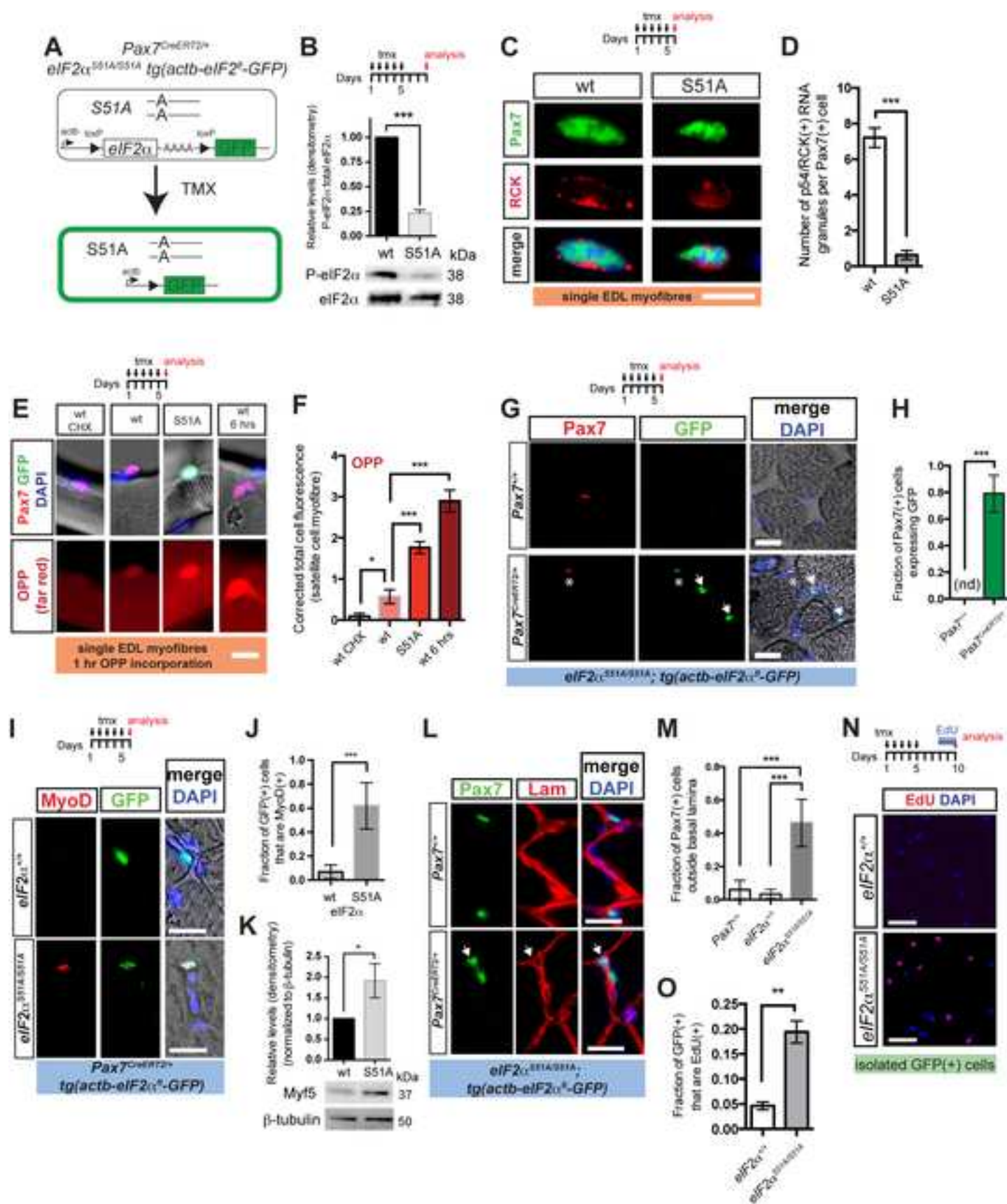


Figure 3

[Click here to download Figure: Figure 3\\_v1.tif](#)

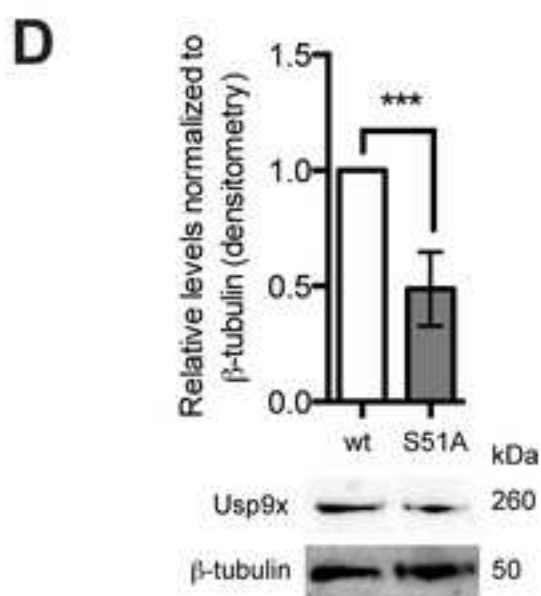
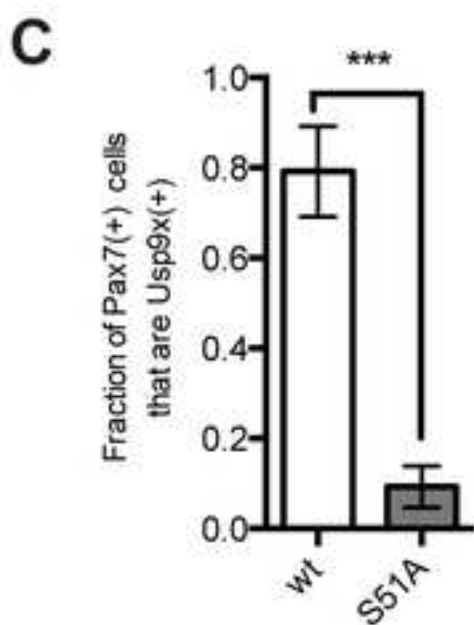
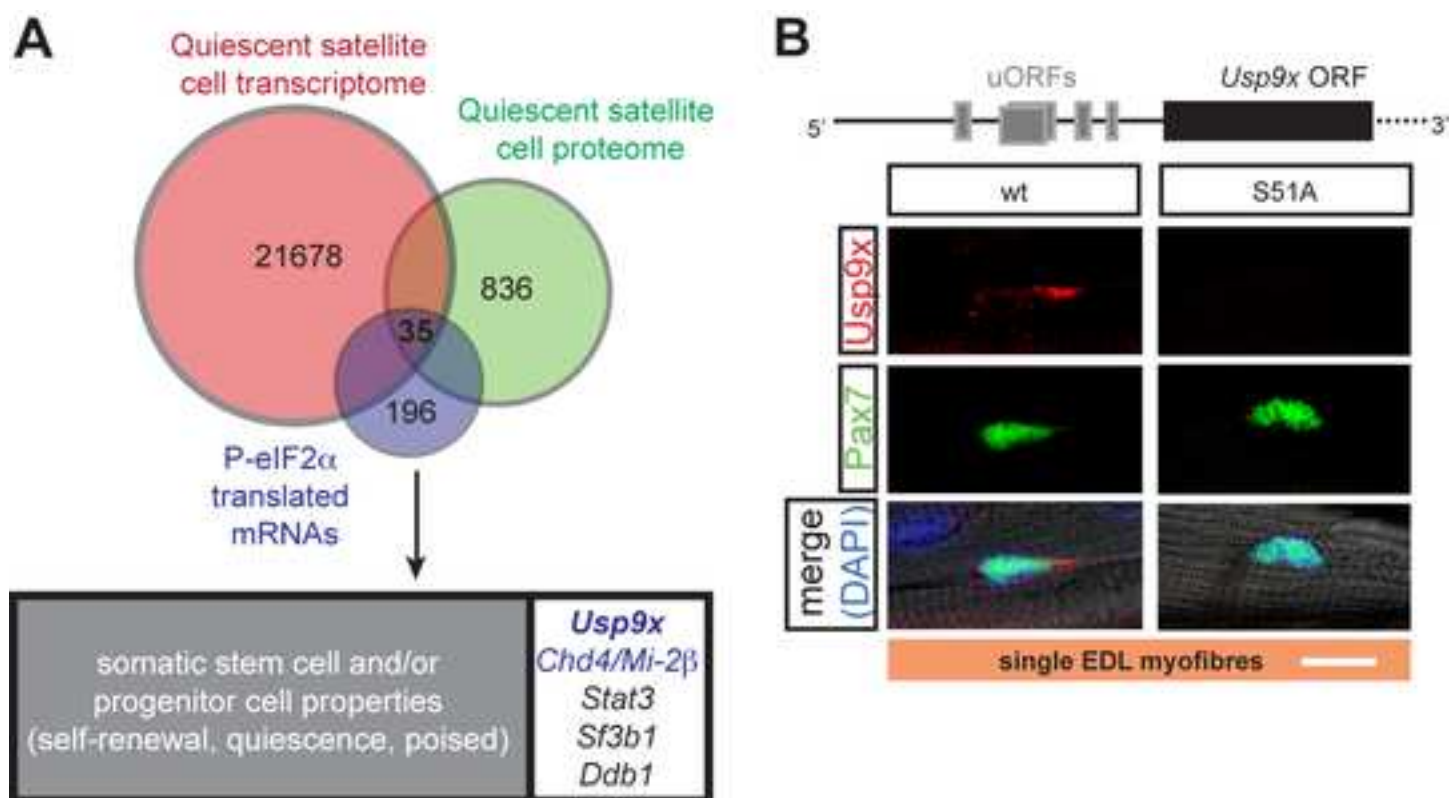


Figure 4  
[Click here to download Figure: Figure 4\\_v2.tif](#)

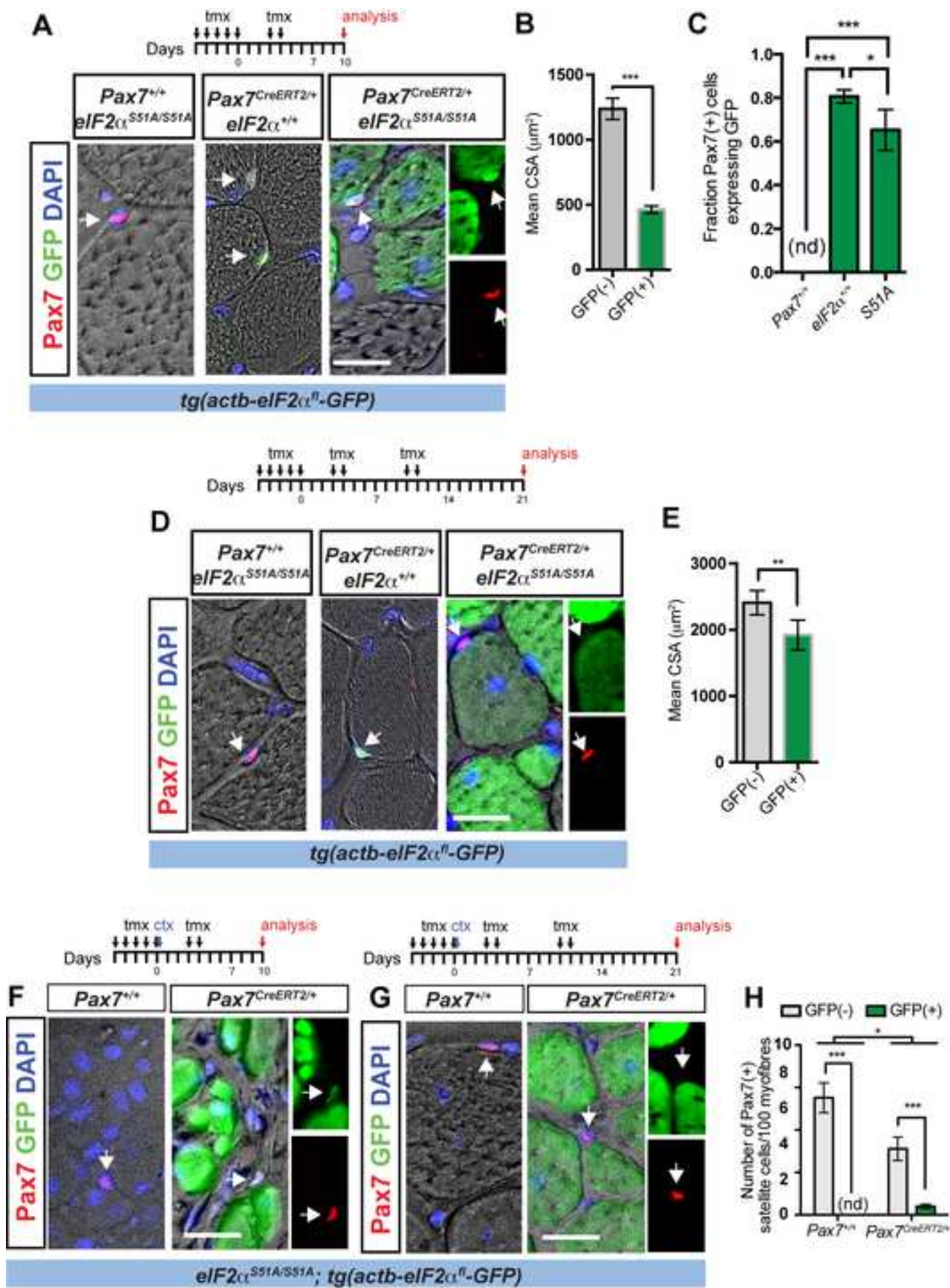


Figure 5

[Click here to download Figure: Figure 5\\_revisedv1.tif](#)

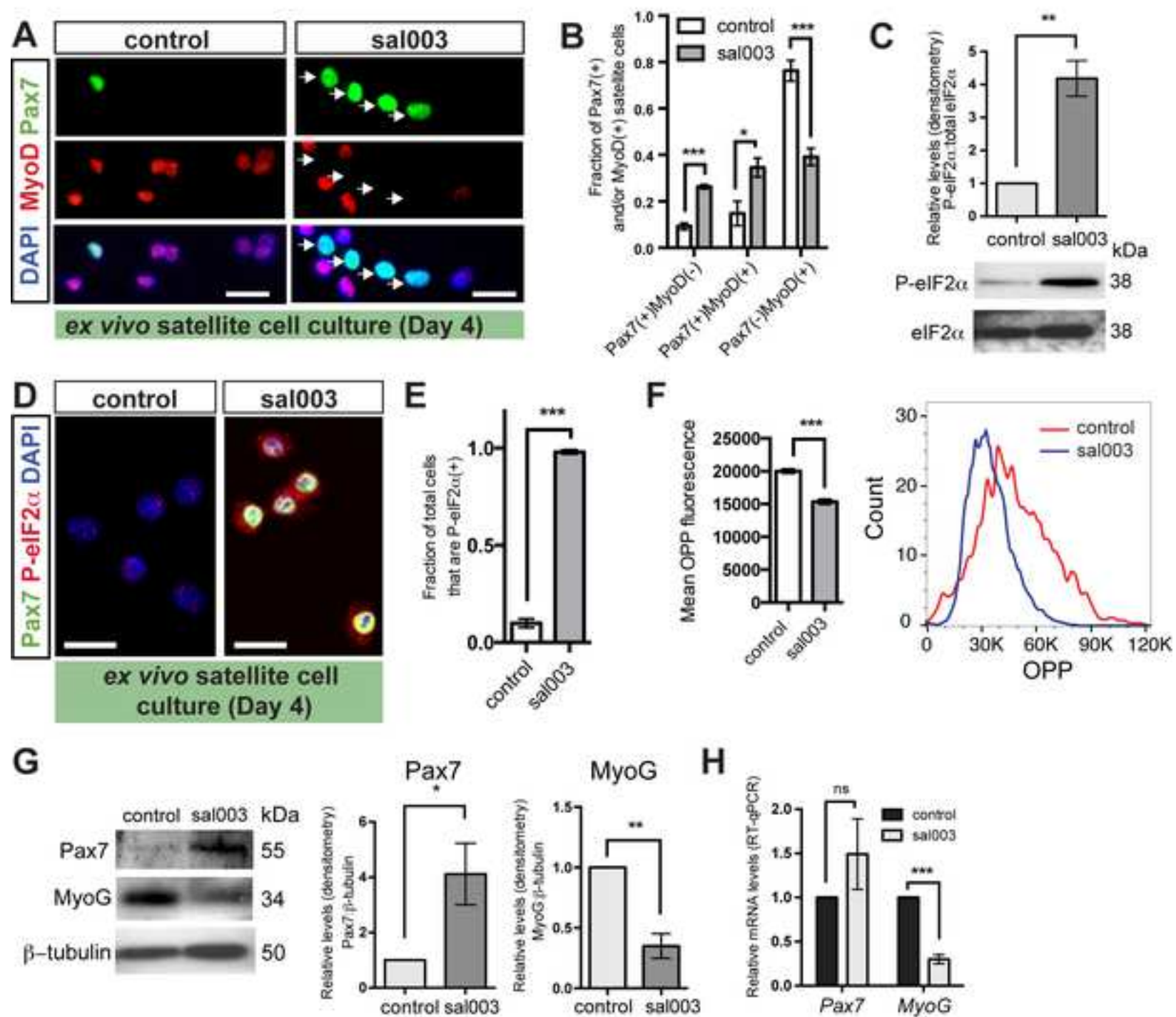
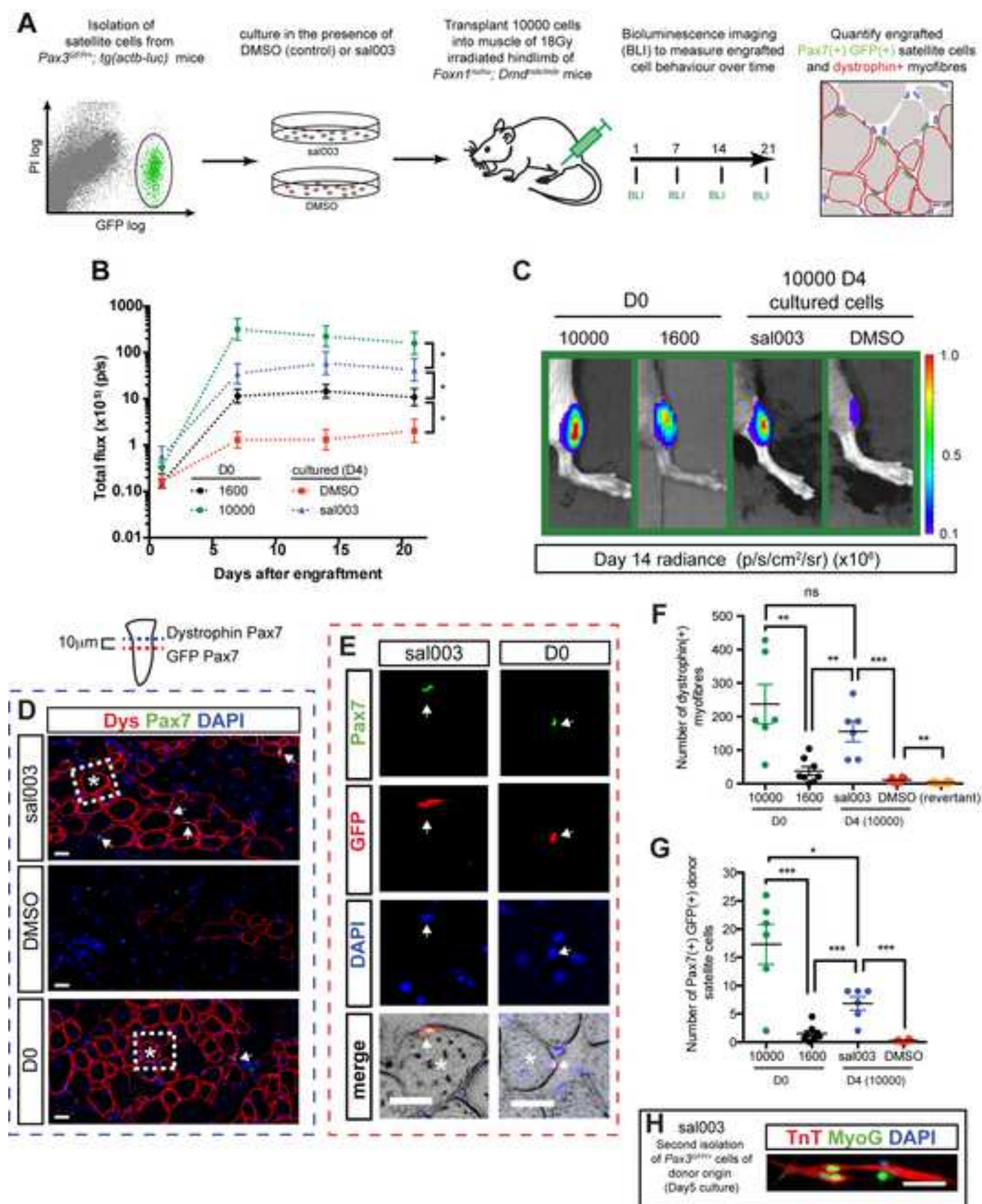
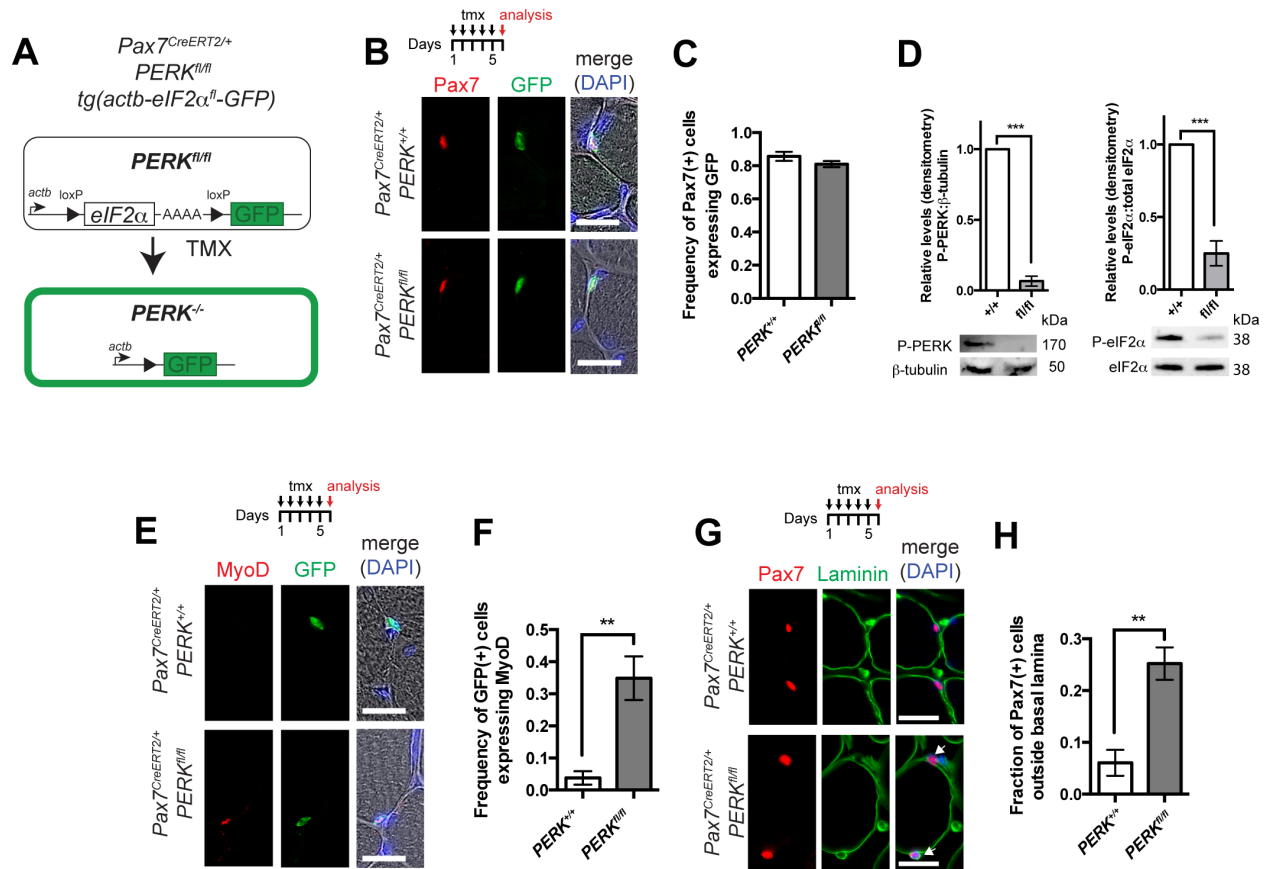


Figure 6  
[Click here to download Figure: Figure 6.tif](#)



## SUPPLEMENTAL FIGURE LEGENDS

## Figure S1



**Figure S1. Satellite Cells Deficient for PERK do not Phosphorylate eIF2α and Enter the Myogenic Program *in vivo*, related to Figure 2.**

(A) *Pax7<sup>CreERT2/+</sup>* mice crossed with *PERK<sup>fl/fl</sup>* allows the conditional deletion of *PERK* in Pax7(+) satellite cells after tmx administration. The transgene with floxed wild-type *eIF2α* under the control of CMV enhancer and chicken β-actin promoter (*actb*) upstream of a GFP reporter (green) is maintained in this mouse line to identify GFP-positive cells.

(B) Immunostaining for Pax7 (red) and GFP (green) on transverse sections of TA muscle after 5 daily doses of tmx (indicated). Right panels show merged images with DAPI, which are overlaid on brightfield images of transverse fibre sections.

(C) Fraction of Pax7(+) nuclei that show immunofluorescence for GFP indicated in (B).

(D) Immunoblotting for P-PERK,  $\beta$ -tubulin, P-eIF2 $\alpha$  and total eIF2 $\alpha$  of cell lysates from newly isolated GFP(+) cells from muscle of tmx treated *Pax7<sup>CreERT2/+</sup>*, *tg(actb-eIF2 $\alpha^fl$ -GFP)*, *PERK<sup>fl/fl</sup>* (fl/fl) and wild-type *PERK<sup>+/+</sup>* (+/+) animals. Relative levels of P-PERK, normalized to  $\beta$ -tubulin and P-eIF2 $\alpha$ , normalized to total eIF2 $\alpha$  are indicated, with representative immunoblots.

(E) Immunostaining MyoD (red) and GFP (green) on transverse sections of TA muscle after tmx treatment. Right panels are merged images with DAPI, overlaid on brightfield to show myofibres.

(F) Fraction of GFP(+) cells that are MyoD(+) in (E).

(G) Immunostaining Pax7 (red) and Laminin (green) on transverse sections of TA muscle after tmx treatment. Right panels show merged images with DAPI. Arrows indicate position of satellite cells outside basal lamina.

(H) Fraction of Pax7(+) nuclei outside the basal lamina of myofibres after tmx treatment indicated in (G).

Scale bars, 50 $\mu$ m. All values indicate mean (n $\geq$ 3)  $\pm$  s.e.m. \*\*  $p < 0.01$ , \*\*\*  $p < 0.001$ .

**Figure S2**

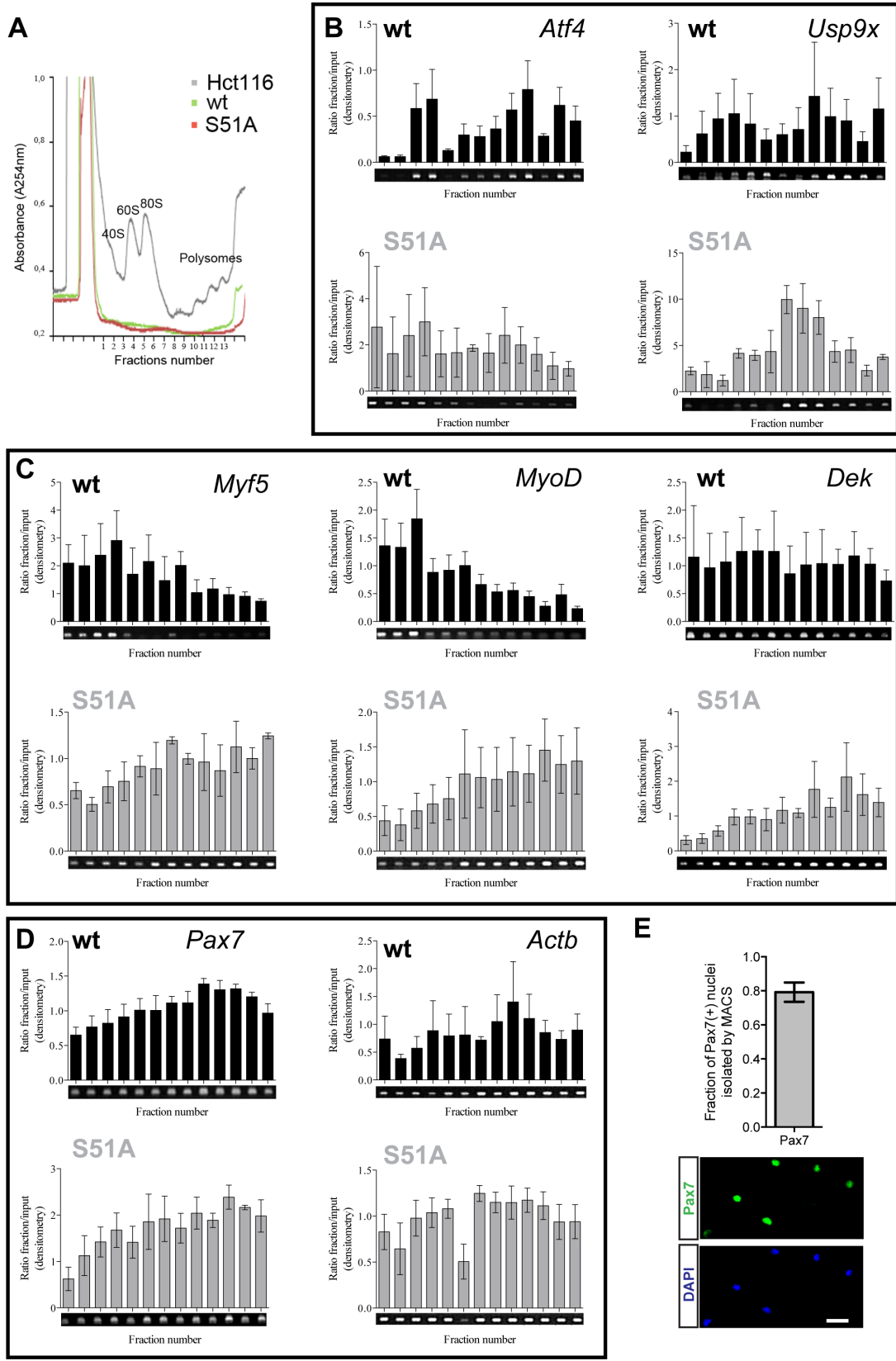


**Figure S2. P-eIF2 $\alpha$  dependent changes in polysome association of transcripts from satellite cell lysates after sucrose gradient centrifugation, related to Figure 3.**

(A) Fractions were collected by sucrose gradient analyses of lysates prepared from >300 000 wild-type (*eIF2 $\alpha$ <sup>+/+</sup>*, green) S51A (*eIF2 $\alpha$ <sup>S51A/S51A</sup>*, red) satellite cells and  $1 \times 10^7$  Hct116 cells (blue).

(B) Transcripts sensitive to eIF2 $\alpha$  phosphorylation, determined by increased association with heavy polysome fractions isolated from S51A satellite cells.

(C) Transcripts selectively translated when eIF2 $\alpha$  is phosphorylated in quiescent satellite cells, determined by decreased association with heavy polysome fractions, or increased association with light fractions isolated from S51A satellite cells.

(D) Transcripts resistant to eIF2 $\alpha$  phosphorylation in quiescent satellite cells, determined by continued association with heavy polysome fractions.

All values indicate mean ( $n \geq 3$ )  $\pm$  s.e.m. and images of representative fractionations are shown.

(E) Polysome analysis is performed on lysates of satellite cells isolated by enzymatic dissociation of muscle followed by magnetic separation. Frequency of Pax7(+) nuclei is shown, with a representative image of immunostaining for Pax7 (green) on freshly isolated cells. DAPI nuclear stain is shown (blue). Value indicates mean ( $n \geq 3$ )  $\pm$  s.e.m. of three independent isolations. Scale bar, 20 $\mu$ m.

**Figure S3**

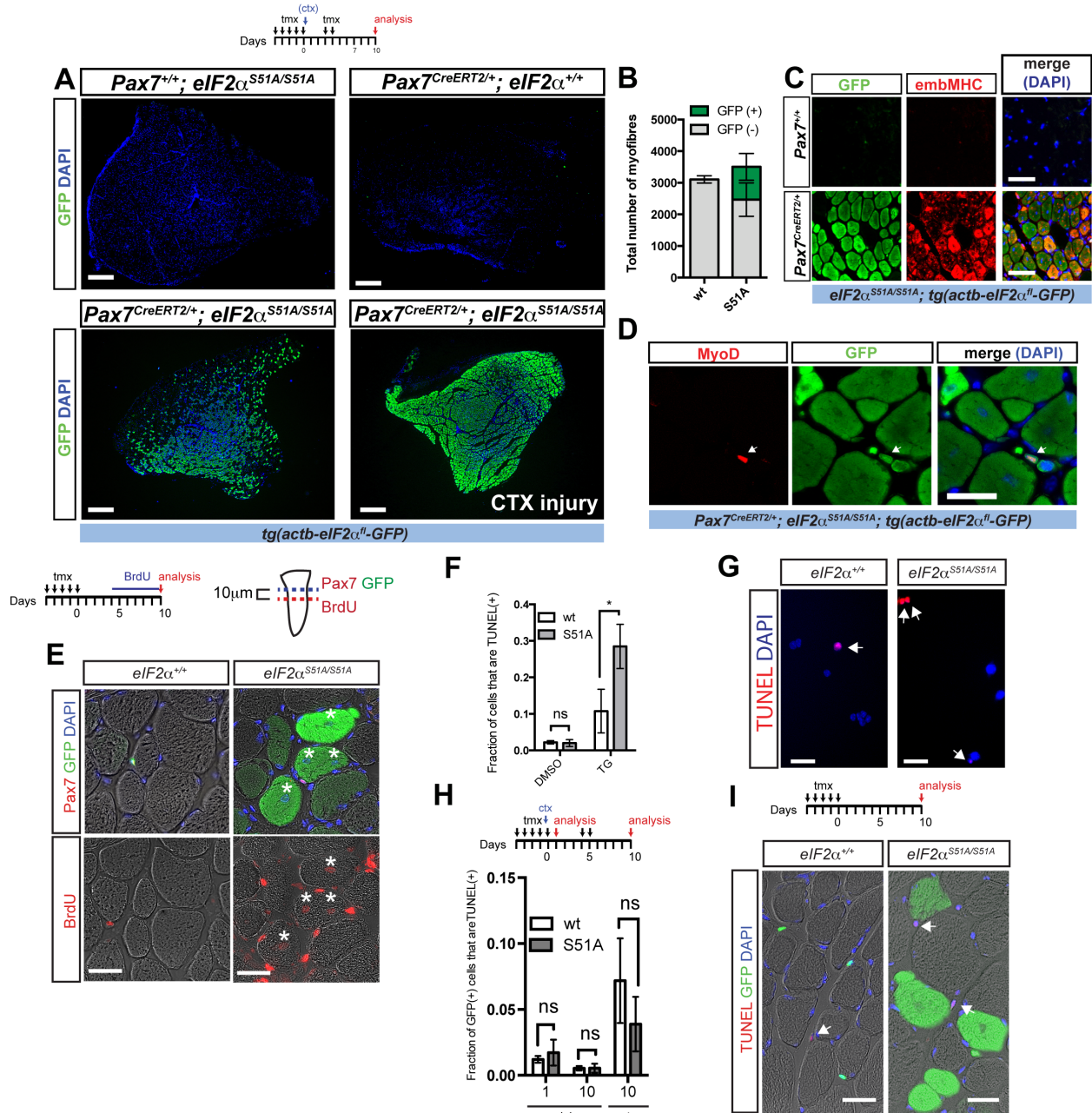


**Figure S3. Activated S51A satellite cells contribute to newly generating muscle fibres, related to Figure 4.**

(A) Low magnification images of transverse sections of TA muscle shown in Figure 3A-B, after immunolabeling for GFP, 10 days after tmx administration (left) and after ctx injury (right) of

either *Pax7*<sup>+/+</sup>, *tg(actb-eIF2 $\alpha$ <sup>fl</sup>-GFP); eIF2 $\alpha$ <sup>S51A/S51A</sup>* control (upper panels) and *Pax7*<sup>CreERT2/+</sup>, *tg(actb-eIF2 $\alpha$ <sup>fl</sup>-GFP); eIF2 $\alpha$ <sup>S51A/S51A</sup>* (S51A) (lower panels).

(B) Total number of myofibres that are GFP(-) or GFP(+) 10 days after tmx administration in uninjured muscle shown in (A, left panels).

(C) Immunostaining for GFP (green) and embryonic myosin heavy chain (embMHC, red) 10 days after tmx administration of either *Pax7*<sup>+/+</sup>, *tg(actb-eIF2 $\alpha$ <sup>fl</sup>-GFP); eIF2 $\alpha$ <sup>S51A/S51A</sup>* control (upper panels) and *Pax7*<sup>CreERT2/+</sup>, *tg(actb-eIF2 $\alpha$ <sup>fl</sup>-GFP); eIF2 $\alpha$ <sup>S51A/S51A</sup>* (S51A) (lower panels). Merged images with DAPI (blue) and overlaid on brightfield images showing myofibres are shown.

(D) Immunostaining transverse sections of TA muscle for MyoD (red) and GFP (green), 10 days after tmx administration of *Pax7*<sup>CreERT2/+</sup>, *tg(actb-eIF2 $\alpha$ <sup>fl</sup>-GFP); eIF2 $\alpha$ <sup>S51A/S51A</sup>* mice. Arrow indicates MyoD(+), GFP(+) cell.

(E) Immunostaining transverse sections of TA muscle for Pax7 (red) and GFP (green), 10 days after tmx administration of *Pax7*<sup>CreERT2/+</sup>, *tg(actb-eIF2 $\alpha$ <sup>fl</sup>-GFP); eIF2 $\alpha$ <sup>S51A/S51A</sup>* mice, with adjacent sections immunostained for BrdU. Asteriks, central nucleated BrdU(+) myofibres.

(F) TUNEL assay after four day culture of satellite cells isolated from tmx treated *Pax7*<sup>CreERT2/+</sup>, *tg(actb-eIF2 $\alpha$ <sup>fl</sup>-GFP); eIF2 $\alpha$ <sup>+/+</sup>* (wt) and *eIF2 $\alpha$ <sup>S51A/S51A</sup>* mice (S51A). DMSO (control) and thapsigargin (TG) were added to culture conditions for 12 hours prior to analysis.

(G) Representative images of satellite cell cultures after addition of TG for 12 hours, as in (F). Arrows indicate TUNEL(+) cells.

(H) TUNEL assay on transverse sections of TA muscle after tmx administration to *Pax7*<sup>CreERT2/+</sup>, *tg(actb-eIF2 $\alpha$ <sup>fl</sup>-GFP); eIF2 $\alpha$ <sup>+/+</sup>* (wt) and *eIF2 $\alpha$ <sup>S51A/S51A</sup>* mice with and without injury. Days of analysis are indicated.

(I) Representative transverse sections of TA muscle immunostained for GFP (green), combined with TUNEL assay, 10 days after tmx administration to *Pax7<sup>CreERT2/+</sup>*, *tg(actb-eIF2 $\alpha^f$ -GFP)*; *eIF2 $\alpha^{+/+}$*  and *eIF2 $\alpha^{S51A/S51A}$*  mice. Arrows indicate TUNEL(+) cells.

Scale bars, 50 $\mu$ m, except in (A), 500 $\mu$ m and (G), 20 $\mu$ m. All values indicate mean (n $\geq$ 3)  $\pm$  s.e.m.

\*  $p < 0.05$ , ns, not significant.

**Figure S4**

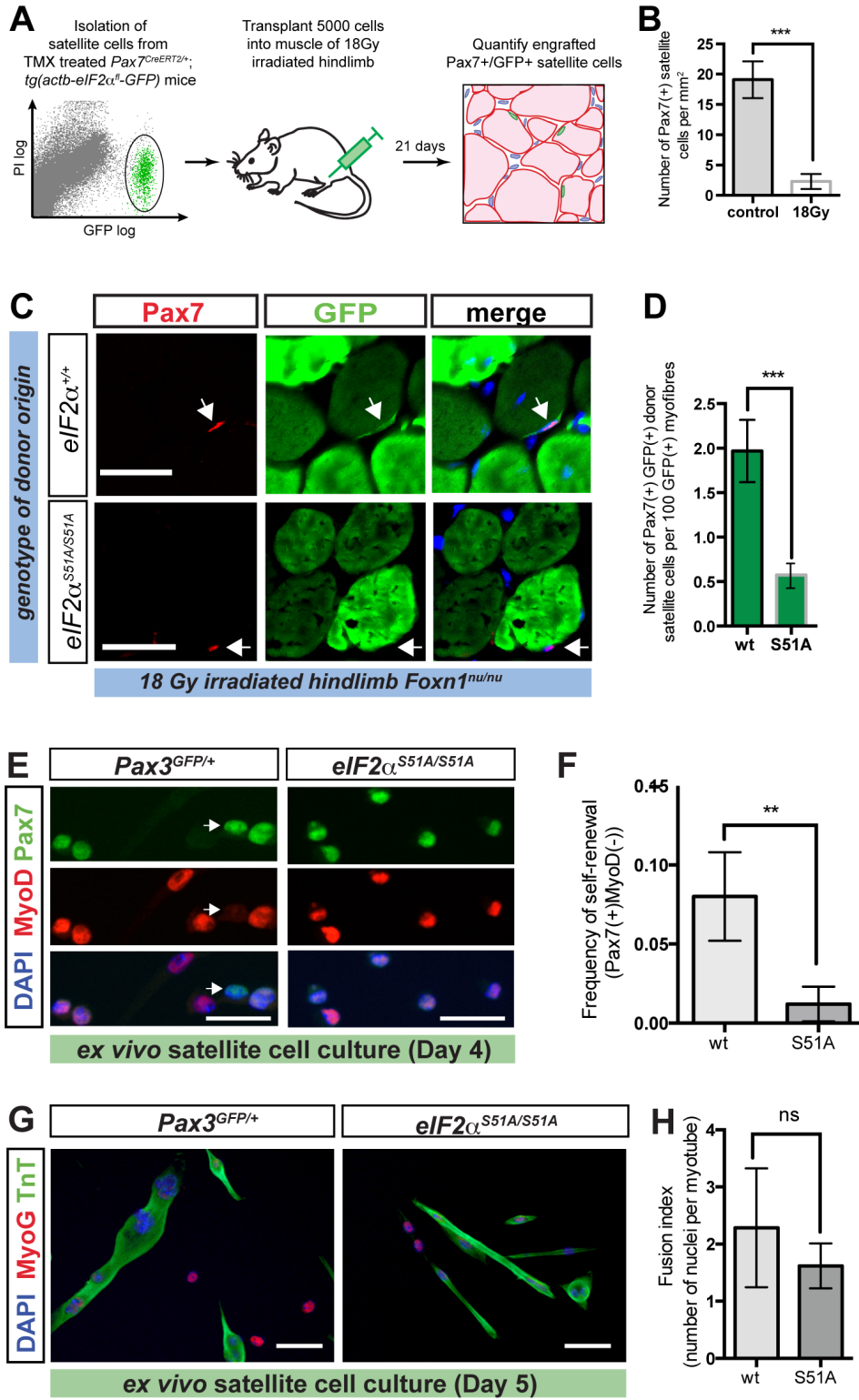


**Figure S4. S51A Satellite Cells Have Diminished Self-Renewal Capacity, related to Figure 4.**

(A) Schematic representation of donor satellite cell isolation from muscle of tmx treated

*Pax7<sup>CreERT2/+</sup>; tg(actb-eIF2 $\alpha^{\text{fl}}$ -GFP); eIF2 $\alpha^{+/+}$*  (control) and *Pax7<sup>CreERT2/+</sup>; tg(actb-eIF2 $\alpha^{\text{fl}}$ -GFP); eIF2 $\alpha^{\text{S51A/S51A}}$*  (S51A) mice and engraftment into the TA muscle of 18Gy-irradiated hindlimbs of 6 week old *Foxn1<sup>mut/mut</sup>* mice. Donor satellite cell contribution to self-renewal was monitored by the presence of Pax7(+), GFP(+) (green) satellite cells on transverse sections of TA muscle, 3 weeks after engraftment.

(B) Number of endogenous Pax7(+) satellite cells remaining 2 days after 18Gy hindlimb irradiation, compared to non-irradiated contralateral controls. Values are mean and s.e.m. taken from n>10 transverse sections of TA muscles isolated from 3 independently irradiated mice.

(C) Immunostaining against Pax7 (red) and GFP (green), merged with DAPI (blue) on transverse sections of TA muscle, 21 days after engraftment with newly isolated satellite cells from tmx treated *Pax7<sup>CreERT2/+</sup>; tg(actb-eIF2 $\alpha^{\text{fl}}$ -GFP); eIF2 $\alpha^{+/+}$*  (control) and *Pax7<sup>CreERT2/+</sup>; tg(actb-eIF2 $\alpha^{\text{fl}}$ -GFP); eIF2 $\alpha^{\text{S51A/S51A}}$*  (S51A) mice. Arrows indicate location of Pax7(+) satellite cells of donor origin (GFP(+), upper panels) and host-origin (GFP(-), lower panels). Scale bars, 50 $\mu\text{m}$ .

(D) Numbers (mean  $\pm$  s.e.m.) of Pax7(+) satellite cells of donor (GFP(+)), per 100 GFP(+) myofibres, 21 days after engraftment.

(E) Immunostaining with antibodies against Pax7 (green) and MyoD (red) of satellite cells isolated from muscle of *Pax3<sup>GFP/+</sup>* or tmx treated *Pax7<sup>CreERT2/+</sup>; tg(act-eIF2 $\alpha^{\text{fl}}$ -GFP); eIF2 $\alpha^{\text{S51A/S51A}}$*  mice after *ex vivo* culture for 4 days. Arrow indicates position of Pax7(+), MyoD(-) reserve cell. Scale bars, 20 $\mu\text{m}$ .

(F) Frequency of self-renewal, as reported by fraction of Pax7 and/or MyoD positive nuclei that are Pax7(+), MyoD(-) reserve cells. All values indicate mean (n≥3) ± s.e.m. \*\*  $p < 0.01$ , (ns, not significant).

(G) Immunostaining against MyoG (red) and TroponinT (TnT, green) of satellite cells isolated from muscle of  $Pax3^{GFP/+}$  or tmx treated  $Pax7^{CreERT2/+}; tg(act-eIF2\alpha^{fl}-GFP); eIF2\alpha^{S51A/S51A}$  mice after *ex vivo* culture for 5 days. Scale bars, 20µm.

(H) Fusion index, or number of myonuclei per TroponinT(+) myotube of differentiated satellite cells isolated from muscle of  $Pax3^{GFP/+}$  or tmx treated  $Pax7^{CreERT2/+}; tg(act-eIF2\alpha^{fl}-GFP); eIF2\alpha^{S51A/S51A}$  mice after *ex vivo* culture for 5 days.

All values indicate mean (n≥3) ± s.e.m. \*\*  $p < 0.01$ , \*\*\*  $p < 0.001$ , ns, not significant.

**Figure S5**

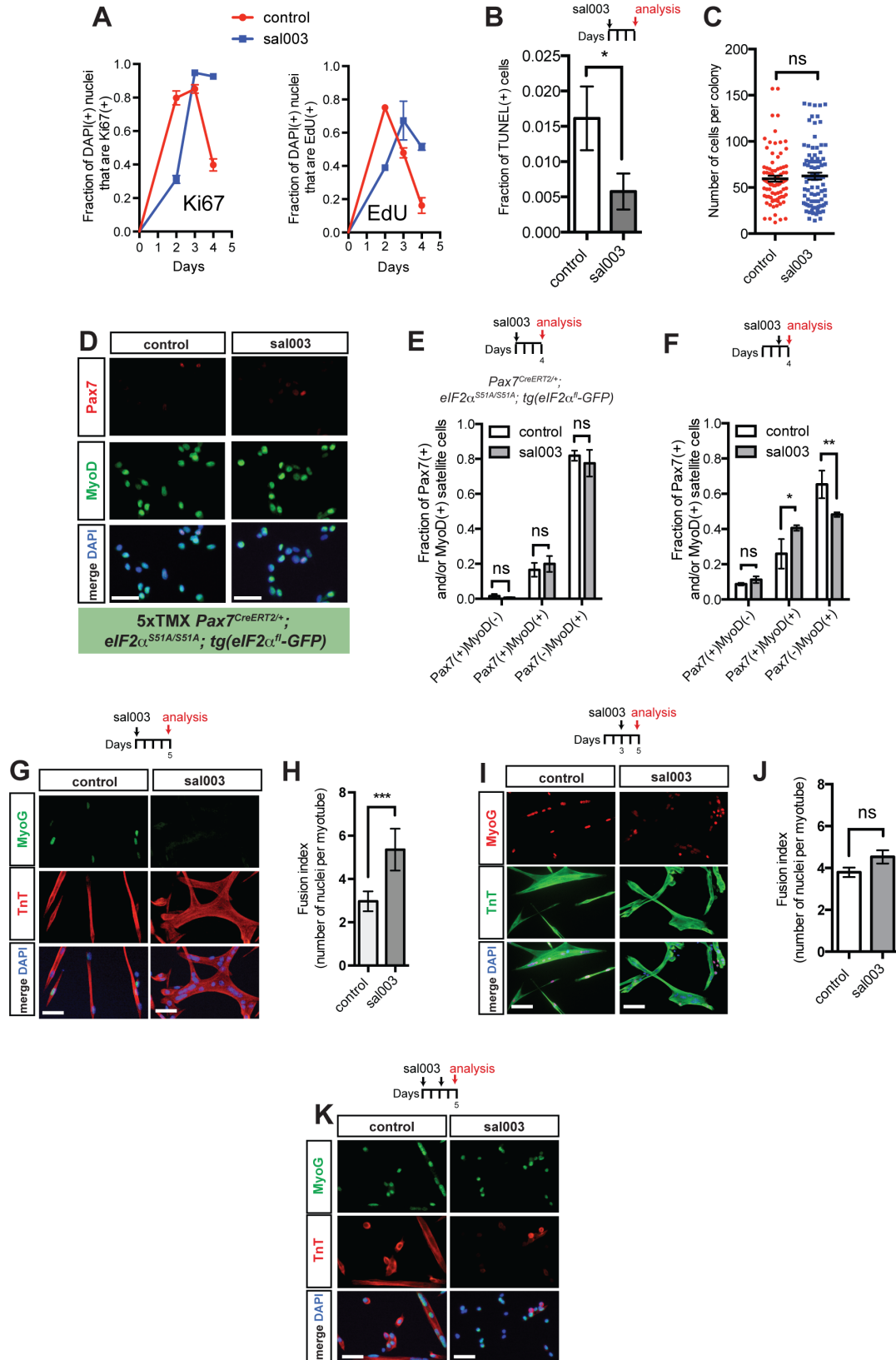


**Figure S5. The effect of sal003 to promote self-renewal and delay differentiation requires eIF2 $\alpha$  phosphorylation and is transient, related to Figure 5.**

(A) Ki67 (left) and EdU (right) labeling of satellite cells during culture in the presence of DMSO (control) and sal003.

(B) TUNEL labeling of satellite cells after 4 day culture in the presence of DMSO (control) and sal003.

(C) Total cells per colony, measured by DAPI positive nuclei, after 4 day culture in the presence of DMSO (control) and sal003.

(D) Immunostaining against Pax7 (red) and MyoD (green) of satellite cells isolated from muscle of TMX treated *Pax7<sup>CreERT2/+</sup>; eIF2 $\alpha$ <sup>S51A/S51A</sup>, tg(eIF2 $\alpha$ <sup>fl</sup>-GFP)* mice and cultured *ex vivo* with DMSO (control) or sal003 for 4 days. Merged images with DAPI are shown (bottom panel).

(E) Frequency of self-renewal (Pax7(+)MyoD(-)), activation (Pax7(+)MyoD(+)) and differentiating (Pax7(-)MyoD(+)) S51A cells after 4 day culture with DMSO (control) or sal003.

(F) Frequency of self-renewal (Pax7(+)MyoD(-)), activation (Pax7(+)MyoD(+)) and differentiating (Pax7(-)MyoD(+)) cells after 4 day culture with addition of DMSO (control) or sal003 at day 3.

(G) Immunostaining against MyoG (green) and TroponinT (TnT, red) of satellite cells isolated from muscle of *Pax3<sup>GFP/+</sup>* and cultured *ex vivo* with DMSO (control) or sal003 for 5 days. Merged images with DAPI are shown (bottom panel).

(H) Fusion index, or number of myonuclei per TroponinT(+) myotube after 5 day culture *ex vivo* of satellite cells with DMSO (control) or sal003 as shown in (D).

(I) Immunostaining against MyoG (red) and TroponinT (TnT, green) after 5 day culture *ex vivo* of satellite cells with DMSO (control) and sal003 added at day 3, as indicated.

(J) Fusion index, after 5 day culture *ex vivo* of satellite cells with DMSO (control) or sal003 added at day 3, as shown in (I).

(K) Immunostaining against MyoG (green) and TroponinT (TnT, red) after media was replenished at day 3 with DMSO (control) and sal003, as indicated.

Scale bars, 20 $\mu$ m. Values indicate mean ( $n \geq 3$ )  $\pm$  s.e.m. \*  $p < 0.05$ , \*\*  $p < 0.01$ , \*\*\*  $p < 0.001$ , ns, not significant.

SUPPLEMENTAL TABLE

Table S1. Candidate mRNAs selectively translated in the quiescent satellite cell, related to Figure 3.

Gene Symbol	uORFs <sup>a</sup>	Description
<b>RNA binding</b>		
<i>Qars</i>	2	glutaminyl-tRNA synthetase
<i>Dhx9</i>	1	DEAH (Asp-Glu-Ala-His) box polypeptide 9
<i>Prpf8</i>	1	pre-mRNA processing factor 8
<i>Lrpprc</i>	1	leucine-rich PPR-motif containing
<i>Vars</i>	0	Valyl-tRNA synthetase
<i>Ganab</i>	0	alpha glucosidase 2 alpha neutral subunit
<i>Sf3b1</i>	0	Splicing factor 3B subunit 1
<i>Eif3a</i>	0	eukaryotic translation initiation factor 3, subunit A
<i>Rrbp1</i>	0	ribosome binding protein 1
<i>Eprs</i>	0	glutamyl-prolyl-tRNA synthetase
<i>Cyfipl</i>	0	cytoplasmic FMR1 interacting protein 1
<b>DNA binding</b>		
<i>Tpr</i>	2	translocated promoter region, nuclear basket protein
<i>Chd4</i>	1	Chromodomain-helicase-DNA-binding protein 4
<i>Pds5b</i>	1	PDS5, regulator of cohesion maintenance, homolog B ( <i>S. cerevisiae</i> )
<i>Hcfc1</i>	1	host cell factor C1
<i>Smc3</i>	1	Structural maintenance of chromosomes protein 3
<i>Ddb1</i>	0	damage specific DNA binding protein 1
<i>Stat3</i>	0	Signal transducer and activator of transcription 3
<i>Mybbp1a</i>	0	MYB binding protein (P160) 1a
<i>Snd1</i>	0	Staphylococcal nuclease domain-containing protein 1
<b>Protein modification</b>		
<i>Usp9x</i>	5	ubiquitin specific peptidase 9, X chromosome
<i>Npepps</i>	0	aminopeptidase puromycin sensitive
<b>Metabolism</b>		
<i>Hkl</i>	2	hexokinase 1
<i>Aco2</i>	2	Aconitase 2, mitochondrial
<i>Acly</i>	1	ATP citrate lyase
<i>Asph</i>	0	Aspartate Beta-Hydroxylase
<i>Hadha</i>	0	hydroxyacyl-CoA dehydrogenase/3-ketoacyl-CoA thiolase/enoyl-CoA hydratase, alpha
<i>Gpd2</i>	0	glycerol phosphate dehydrogenase 2, mitochondrial
<b>Cell interactions</b>		
<i>Tjp1</i>	1	Tight junction protein 1
<i>Vcl</i>	0	Vinculin
<i>Myof</i>	0	Myoferlin
<b>Other</b>		
<i>Glg1</i>	5	Golgi complex-localized glycoprotein 1
<i>Spcb2</i>	3	spectrin beta 2
<i>Iqgap1</i>	1	IQ motif containing GTPase activating protein 1
<i>Cltc</i>	0	Clathrin heavy chain 1

<sup>a</sup>(from Baird et al. 2014)

## **SUPPLEMENTAL EXPERIMENTAL PROCEDURES**

### **Care and handling of mice**

Care and handling of animals were in accordance with the federal Health of Animals Act, as practiced by McGill University and the Lady Davis Institute for Medical Research.

For satellite cell engraftment, host mice were anesthetised with rodent cocktail (ketamine (100mg/kg) xylazine (10mg/kg) and acepromazine (3mg/kg)) and hindlimbs were irradiated with 18 Gy of 180 kVp x-rays one day prior to engraftment. Immediately prior to engraftment, donor cells were counted with a haemocytometer, with non-viable cells excluded by 0.4% Trypan Blue stain (Gibco). Donor satellite cells were centrifuged for 20 minutes at  $700 \times g$ ,  $4^{\circ}\text{C}$  and resuspended in DMEM media (Life Technologies) prior to engraftment into the TA muscle by  $5\mu\text{l}$  microcapillary pipette (Drummond). For live animal bioluminescence imaging (BLI), donor cells were obtained from *tg(actb-luc)* animals (Taconic) and imaging was performed with an IVIS Spectrum *in vivo* imaging system (Perkin Elmer). D-luciferin (Gold Biotechnology) was administered by two  $100\mu\text{l}$  contralateral intraperitoneal injections to give a final dose of 150mg/kg. 20 minutes after D-luciferin administration mice were anesthetized with isoflurane prior to imaging and data acquisition.

### **Protein Analysis**

Primary antibodies were against Pax7 (monoclonal, DSHB; polyclonal, Aviva Systems Biology ARP32742\_P050), Myf5 (Santa Cruz, sc-302), MyoD (monoclonal Dako, M3512; polyclonal SantaCruz, sc-304), MyoG (Santa-Cruz, sc-576), TroponinT (Sigma, T6277), embryonic MHC (DSHB, F1.652), Dystrophin (Thermo Scientific, PA1-37587), P-eIF2 $\alpha$  (Novus, NB110-56949), total eIF2 $\alpha$  (Cell Signaling, 3179), P-PERK (Cell Signaling, 3179), ATF4 (Novus, H468-M01),

CHOP (Novus, NB600-1335), BiP (Cell Signaling, 3183), Ki67 (BD Biosciences B56), BrdU (BD Pharmingen, 555627), Usp9x (Cell Signaling, 14898), and  $\beta$ -tubulin (Millipore, 05-661).

Alexa Fluor-488 and -594 conjugated secondary anti-mouse or anti-rabbit antibodies (Life Technologies) were used for immunofluorescence and images were acquired with an AxioImager M1 fluorescence microscope (Zeiss). Horseradish peroxidase (HRP) conjugated goat anti-mouse or anti-rabbit secondary antibodies (Jackson ImmunoResearch) were used with the ECL Prime Western Blotting Detection reagents (GE Healthcare) to image immunoblots with ImageQuant LAS 4000 (GE Healthcare).

Protein synthesis was analyzed by OPP incorporation. Freshly isolated or 5 hour cultured single EDL myofibres were cultured for an additional hour at 37°C in the presence of OPP (Medchem Source) at a final concentration of 50 $\mu$ M. EDL myofibres cultured in the presence of CHX (100  $\mu$ g/ml) were used as a negative control. EDL myofibres were washed, fixed and permeabilized as described in Methods. OPP was detected by azide-alkyne cycloaddition with the Click-iT Cell Reaction Buffer Kit (Life Technologies). Corrected total cell fluorescence of the OPP signal was determined using ImageJ (Integrated Density – (Area of selected satellite cell  $\times$  Mean fluorescence of background myofibre). Control and sal003 treated satellite cell cultures were cultured for an additional hour at 37°C in the presence of OPP, fixed as described in Methods and permeabilized with 0.1% Saponin (Life Technologies), prior to OPP detection and analysis by flow cytometry using a FACSAriaIII cell sorter (BD Biosciences).

### **RNA Analysis**

For polysome association studies, cold sucrose gradients between 10 to 55% were prepared using an ISCO model 160 Gradient Former. Before harvesting, HCT116 cells were incubated in the

presence of 100 µg/ml CHX and immediately washed with cold PBS containing 100 µg/ml CHX. Fresh isolated satellite cells were similarly treated and washed with CHX. Cells were lysed for 10 minutes on ice with 800 µl of cold lysis buffer (5 mM MgCl<sub>2</sub>, 1% Triton-X100, 100 µg/ml CHX, 1 mM DTT, 100 unit/ml RNase inhibitor, 15 mM Tris-HCl pH 8.0, 300 mM NaCl). After centrifugation at 16,000×G for 10 min, lysates were layered over the sucrose gradients and centrifuged at 39000 rpm in a Beckman SW40Ti rotor for 3 hours at 4 °C. 13 fractions (0.75 ml/fraction) were collected for RNA isolation and analysis. 500 µg of RNA from each fraction was reverse transcribed using iScript Reverse Transcription Supermix (BioRad).

RT-PCR primers were Pax7 forward 5'-AGGCCTTCGAGAGGACCCAC-3' reverse 5'-CTGAACCAGACCTGGACGCG-3', MyoG forward 5'-CAACCAGGAGGAGCGCGATCTCCG-3' and reverse 5'-AGGCGCTGTGGGAGTTGCATTCAC-3', Dek forward 5'-CGAGAAGGAACCCGAGATG-3' reverse 5'-GGAAGACACTTGCATCGTCA-3', Myf5 forward 5'-CTGTCTGGTCCCGAAAGAAC-3' reverse 5'-AAGCAATCCAAGCTGGACAC-3', MyoD forward 5'-CCCCGGCGGCAGAATGGCTACG-3' reverse 5'-GGTCTGGGTTCCCTGTTCTGTGT-3', Atf4 forward 5'-GCCAGATGAGCTCTTGACCAC-3' reverse 5'-CTGGAGTGGAAGACAGAACCC-3', Usp9x forward 5'-TCCAACAGAATCAGACTTCATCG-3' reverse 5'-TGGAAATGCAGGTTCCCTCATCT-3' and Actb 5'-AAACATCCCCCAAAGTTCTAC-3' and reverse 5'-GAGGGACTTCCTGTAACCACT-3'. For semi-quantitative RT-PCR, PCR products were analyzed by ImageJ software. When indicated, levels of mRNA were measured using SYBR Green on a 7500 Fast Real Time PCR System (Applied Biosystems).

### **Bioinformatics Analysis**

To identify mRNAs selectively translated when eIF2 $\alpha$  is phosphorylated, we compared published datasets describing gene expression at the level of transcripts (accession number GSE15155, Pallafacchina et al. 2010) and protein (GSE66822, Zhang et al. 2015) with mRNAs that are selectively translated when eIF2 $\alpha$  is phosphorylated (GSE54581, Baird et al. 2014). Gene expression (transcripts) was derived by the analysis of GSE15155, performed using the Affy package (<http://www.bioconductor.org/packages/release/bioc/html/affy.html>) in R/Bioconductor ([www.bioconductor.org](http://www.bioconductor.org)). For proteomic data, peptides with counts higher than the average (>136 counts in quiescent satellite cells) were selected as our cutoff point.